

KREH1 RNA helicase activity promotes utilization of initiator gRNAs across multiple mRNAs in trypanosome RNA editing

Ashutosh P. Dubey[†], Brianna L. Tylec[†], Amartya Mishra, Katherine Sortino, Runpu Chen, Yijun Sun[✉] and Laurie K. Read^{✉*}

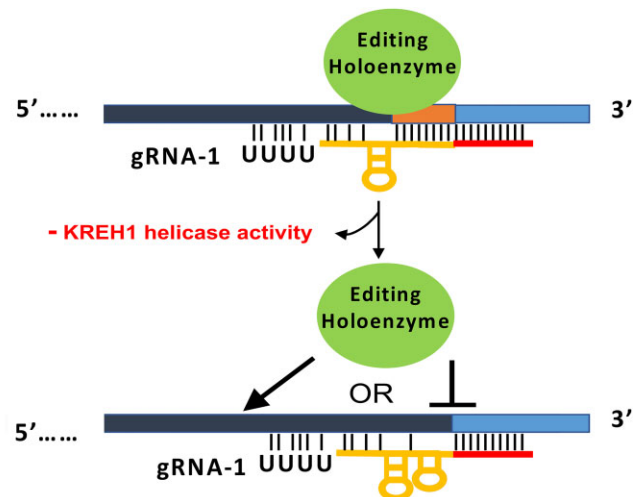
Dept. of Microbiology and Immunology, Jacobs School of Medicine and Biomedical Sciences, Buffalo, NY 14203, USA

Received February 27, 2023; Revised April 04, 2023; Editorial Decision April 09, 2023; Accepted April 11, 2023

ABSTRACT

Mitochondrial U-indel RNA editing in kinetoplastid protozoa is directed by *trans*-acting gRNAs and mediated by a holoenzyme with associated factors. Here, we examine the function of the holoenzyme-associated KREH1 RNA helicase in U-indel editing. We show that KREH1 knockout (KO) impairs editing of a small subset of mRNAs. Overexpression of helicase-dead mutants results in expanded impairment of editing across multiple transcripts, suggesting the existence of enzymes that can compensate for KREH1 in KO cells. In depth analysis of editing defects using quantitative RT-PCR and high-throughput sequencing reveals compromised editing initiation and progression in both KREH1-KO and mutant-expressing cells. In addition, these cells exhibit a distinct defect in the earliest stages of editing in which the initiator gRNA is bypassed, and a small number of editing events takes place just outside this region. Wild type KREH1 and a helicase-dead KREH1 mutant interact similarly with RNA and holoenzyme, and overexpression of both similarly disorders holoenzyme homeostasis. Thus, our data support a model in which KREH1 RNA helicase activity facilitates remodeling of initiator gRNA-mRNA duplexes to permit accurate utilization of initiating gRNAs on multiple transcripts.

GRAPHICAL ABSTRACT



INTRODUCTION

Uridine insertion/deletion (U-indel) RNA editing is an indispensable mechanism for expression of mitochondrially encoded genes in Kinetoplastid protozoa, a group that contains several deadly human parasites (1–6). In *Trypanosoma brucei*, the causative agent of African sleeping sickness, 12 of 18 mitochondrial mRNAs require editing to convert otherwise untranslatable mRNAs into translation competent mRNAs (3–6). U-indel editing is essential for growth of both mammalian and insect stages of the parasite and for virulence in mice (7,8). Two classes of edited mRNAs are distinguished by the numbers of U insertions and deletions needed to generate mature mRNAs. Pan-edited transcripts, such as ND7, COIII and A6, require hundreds of U insertions and dozens of U deletions, while moderately edited transcripts such as CYb and MURF2, require only a few dozen insertions and few or no deletions (9–11). U-indel

*To whom correspondence should be addressed. Tel: +1 716 829 3307; Email: lread@buffalo.edu

[†]The authors wish it to be known that, in their opinion, the first two authors should be regarded as Joint First Authors.

Present address: Amartya Mishra, Division of Infectious Diseases, International Institute of Innovation and Technology, New Town, Kolkata-700156, West Bengal, India.

RNA editing is specified by pairing of mRNAs with small, mitochondrially encoded, *trans*-acting guide RNAs (gRNAs), which then direct editing through interactions involving both Watson–Crick and G–U basepairing (12,13). Editing proceeds through a gRNA-directed block until gRNA and edited mRNA are fully complementary. At this point, the mRNA–gRNA pair is separated by an unknown mechanism, and the next gRNA associates to re-initiate the editing cycle. U-indel RNA editing takes place in a general 3' to 5' direction along the mRNA because editing directed by a given gRNA produces the edited sequence with which the subsequent gRNA forms an anchor duplex. Partially edited transcripts that are in the process of being edited comprise the majority of most edited mRNA populations, as confirmed by numerous high-throughput studies (5,14–21). Although editing proceeds generally 3' to 5', partially edited mRNAs often contain stretches of edited sequence, located between fully edited and pre-edited regions, which are neither pre-edited nor canonically edited. The exact functions and origins of these regions, termed junctions, is a subject of debate; however, it is likely that many junctions represent regions of active editing (5,15,22).

As recently defined (3), the editing holoenzyme is a multiprotein apparatus comprising three dynamically interacting complexes: RNA Editing Catalytic Complex (RECC), RNA Editing Substrate-binding Complex (RESC) and REH2C Complex. Two distinct U insertion RECCs and one U deletion RECC contain the enzymes that catalyze endonuclease cleavage, U insertion/deletion, and RNA ligation (23–25). RESC provides the platform for RNA editing and coordinates interactions between RECC, mRNA, and gRNA. Most RESC proteins lack recognizable domains and are conserved only in kinetoplastids; however, many exhibit RNA binding activity (15,17,19,26–32). RESC itself contains distinct modules, and recent studies identified RESC components that modulate RESC organization, thereby promoting editing initiation and/or 3' to 5' progression (15,19,26,27,33–35). The third component of the editing holoenzyme is REH2C, a complex with three different proteins including the KREH2 ATP dependent RNA helicase that crosslinks with RNA (36). REH2C affects the accuracy of RNA editing in a site-specific and substrate-specific manner on RESC-associated transcripts (4,16). Additional proteins not considered *bona fide* holoenzyme components associate transiently with RECC or RESC and often affect editing of specific mRNAs (20,37–42).

One accessory factor that reportedly plays a role in U-indel editing is KREH1, a DEAD box RNA helicase with RNA unwinding activity that transiently associates with RECC, RESC and REH2C (35,43–48). KREH1 is one of three holoenzyme-associated RNA helicases (KREH1, 2 and 3) (4,47,49), and it is less well studied than KREH2. DEAD box helicases function in a variety of cellular processes requiring RNA–RNA and RNA–protein interactions, and they do so not only by unwinding RNA duplexes, but also through RNA annealing, RNA clamping, RNA structure conversion, and remodeling of RNA–protein (RNP) complexes (50,51). Two previous studies investigated the function of the KREH1 helicase in kinetoplastid RNA

editing. Missel *et al.* (52) showed, using poisoned primer extension, that KREH1 knock out (KO) procyclic form *T. brucei* harbor reduced levels of edited COII and CYb mRNAs. These authors also demonstrated that the bulk of mitochondrial RNA helicase activity does not cofractionate on density gradients with the KREH1 protein. Li *et al.*, (48) subsequently demonstrated the expected ATP dependent RNA unwinding activity of recombinant KREH1 from the related kinetoplastid, *Leishmania tarentolae*. They also provided evidence that KREH1 is involved in the 3' to 5' progression of editing on A6 mRNA, and suggested a role for KREH1 in gRNA removal from an A6 mRNA–gA6 RNA pair, although the latter was not definitively shown (48). Thus, the specific function and mechanism of action of KREH1 helicase in U-indel editing are poorly understood, and the nature of its association with the editing holoenzyme is unclear.

In this present study, we examine KREH1 function in U-indel RNA editing in light of current methodology and our understanding of expanded editing holoenzyme composition. Our sequence analysis of KREH1-KO procyclic *T. brucei* demonstrates that KREH1 promotes RNA editing initiation and influences the Editing Site (ES) at which the initial editing event occurs on A6 transcripts. Analysis of cells expressing dominant negative (DN) helicase-dead KREH1 mutant enzymes demonstrates an expanded role for this enzyme across multiple transcripts, implicating the function of a redundant enzyme in KO cells. Sequence analysis of mRNAs from DN cells, compared to those overexpressing the wild type (WT) enzyme, confirmed results from the KO, revealing impaired initiation and a unique phenotype in which the first editing event takes place 5' of the initiating gRNA, which we term gRNA skipping. Our demonstration of similar protein–protein and protein–RNA interactions in DN compared to WT KREH1 expressors establishes that KREH1 does not function by remodeling of the editing holoenzyme. Instead, our data supports a model in which KREH1 remodels RNA structure to permit the occurrence and proper positioning of U-indel editing initiation.

MATERIALS AND METHODS

Cell line construction and growth

Procyclic form (PF) *T. brucei* strain 29-13, or its derivatives described below, were used for all the experiments. Cells were grown in standard conditions at 27°C in SDM-79 medium supplemented with 10% FBS and 10U/ml of penicillin/streptomycin. Drug concentrations used in this study were 50 µg/ml of puromycin (Invivogen), 15 µg/ml of neomycin (Sigma), 2.5 µg/ml phleomycin (Invivogen), 15 µg/ml hygromycin (Sigma) and 20 µg/ml blasticidin (Invivogen). All primers used in this study are listed in Supplementary Table S1.

KREH1 knock out (KO) cell lines were created by replacement of both alleles with drug resistance cassettes. pKOJET (PURO) and pKOJET (BSD) vectors were created by modification of pJET1.2 (Fermentas) vector by addition of drug resistance cassette as described earlier (53,54). We amplified 500 nt of the KREH1 5' UTR and 3' UTR

sequences and cloned them to flank the resistance genes using primers listed in Supplementary Table S1. First, KREH1 UTR sequences were cloned into pKOJET (PURO), and resulting plasmids were digested with *NotI* and transfected into *T. brucei* 29-13 cells. Transfectants were selected using puromycin, and clones were obtained by limiting dilution. Incorporation of the construct to create single allele KO clones was checked by PCR on genomic DNA using UTR specific primers in Supplementary Table S1. Next, KREH1 UTRs were cloned into pKOJET (BSD), the resulting plasmid was digested and transfected into the selected single KO clones, and transformants were selected with blasticidin. Replacement of both KREH1-KO alleles, resulting in KREH1 null cell lines, was confirmed by PCR using genomic DNA. The KREH2 and RESC8 RNAi lines were previously reported (27,28).

To generate the KREH1 overexpression cell lines, we first used the online tool RecodeTryps (<https://www.acsu.buffalo.edu/~lread/tools.html>) to recode *T. brucei* KREH1 protein-coding sequence for optimal codon usage; this program also recodes the sequence such that the resulting mRNA would be RNAi against the native sequence. The recoded KREH1 DNA sequence was synthesized by GeneScript containing an in-frame C-terminal 6His-TEV-2myc (HTM) tag. KREH1_5'-F and KREH1_3'-R primers containing *BamHI* and *XhoI* sites, respectively, were used to amplify the KREH1 coding sequence and HTM tag. The resulting amplicon was digested with the respective enzymes, gel purified, and ligated into pLEW100, resulting in integration into the rDNA spacer region (55). The resulting pLEW100_KREH1(WT) plasmid was *NotI* digested, purified, and transfected into *T. brucei*. *T. brucei* cells overexpressing DN KREH1 mutants were generated as follows. Site-directed mutagenesis of the codon for lysine 168 (K) to alanine (A) in KREH1 was carried out in the plasmid pLEW100_KREH1(WT) using primers REH1_5'-K168AF and REH1_5'-K168AR (Supplementary Table S1). The same strategy was used to generate a glutamic acid 267 (E) to glutamine (Q) mutation, using primers KREH1_E267Q_For and KREH1_E267Q_Rev (Supplementary Table S1). The correct mutations were confirmed by sequencing, and both KREH1 variants were then transfected into *T. brucei*.

To generate the KREH1-AB (add back) cell line, the pLEW100_KREH1(WT) plasmid described above was *NotI* digested, purified, and transfected into KREH1 null cell lines. For all cells harboring pLEW100-based plasmids, cells were selected with phleomycin and clones obtained by limiting dilution.

In Figure 1C, growth rates were analyzed for one biological replicate each of clones 2 and 3 of KREH1-KO, two biological replicates of WT (i.e. one clone grown two separate times), and three biological replicates each of uninduced and induced KREH1-AB (i.e. one clone grown three separate times uninduced and three separate times induced). In Figure 4, growth rates were analyzed for three biological replicates of each overexpressor cell line (i.e. one clone each grown three separate times). In all cases, three technical replicates were performed for each biological replicate. If error bars are not visible in growth curves, it is due to their small size compared to the symbol.

Generation of tagged cell lines

To generate the cell lines harboring KREH1(WT) or KREH1(KA) in conjunction with a tagged component of the editing holoenzyme (RESC6-ProteinA-Tev-ProteinC (PTP), KREPB5-myc-his-TAP (MHT), or RESC13-10XTy), we proceeded as follows. Cells harboring RESC6-PTP were previously reported (56). KREPB5-MHT was generated by amplifying KREPB5 using the KREPB5-MHT_HindIII_For and KREPB5-MHT_BamHI_Rev primers, digestion of the amplicon with *HindIII* and *BamHI*, and insertion into pHD1034-MHT (26). The resulting pHD1034-KREPB5-MHT was linearized with *NotI* and transfected into 29-13 cells, and cells selected with puromycin and cloned by limiting dilution. Next, we transfected the linearized KREH1(WT) or KREH1(KA) plasmids described above into cell lines expressing RESC6-PTP or KREPB5-MHT, selected with phleomycin and puromycin, and cloned the selected cells by limiting dilution. To generate a cell line harboring RESC13-10XTY and KREH1(WT) or RESC13-10XTY and KREH1(KA), the overexpression cell lines described above were transfected with a 10X-TY-tagging cassette obtained by amplification of the pPOTv4-MHT-blasticidin vector with PCR primers (RESC13_SD-F and RESC13_SD-R) as described earlier (19). Cells were selected with phleomycin and blasticidin, and clones obtained by limiting dilution. All KREH1 overexpressor cell lines were grown in the presence of 4 $\mu\text{g}/\text{mL}$ doxycycline to induce expression of the KREH1 constructs, and western blot with $\alpha\text{-Myc}$ specific antibodies (ICL) was used to confirm similar levels of expression between KREH1 variants relative to the p22 control (41).

qRT-PCR analysis

qRT-PCR analysis of KREH1-KO was performed with one biological replicate each of clones 2 and 3, each with three technical replicates. PF *T. brucei* lines harboring KREH1 WT, KA and EQ overexpression constructs were grown in the presence or absence of 4 $\mu\text{g}/\text{ml}$ doxycycline for 3 days. In both cases, RNA was extracted with TRIzol reagent (Ambion) and treated with DNaseI (Ambion) according to manufacturer's instructions. RNA was purified using phenol/chloroform followed by ethanol precipitation. The purity and quality of the RNA was measured using Nanodrop 1000, and 260/280 ratio was ~ 2 and on a 1.0% of TBE agarose gel, respectively. One μg of RNA was reverse transcribed using random hexamer primers and the iScript reverse transcriptase kit (BioRad). To detect levels of KREH1 mRNA, qRT-PCR was performed using the KREH1 specific primers described in Supplementary Table S1, and *T. brucei* established primers were used to detect levels of pre-edited, edited, and total mitochondrial transcripts, with normalization to 18S rRNA (18,26,27,57). qRT-PCRs were performed using two independent biological replicates, each in technical triplicate, and analyzed by using BioRad iQ5 software.

High-throughput sequencing and bioinformatic analysis

KREH1 WT, KA, and EQ overexpressor cell lines (two biological replicates) were grown in the presence or absence

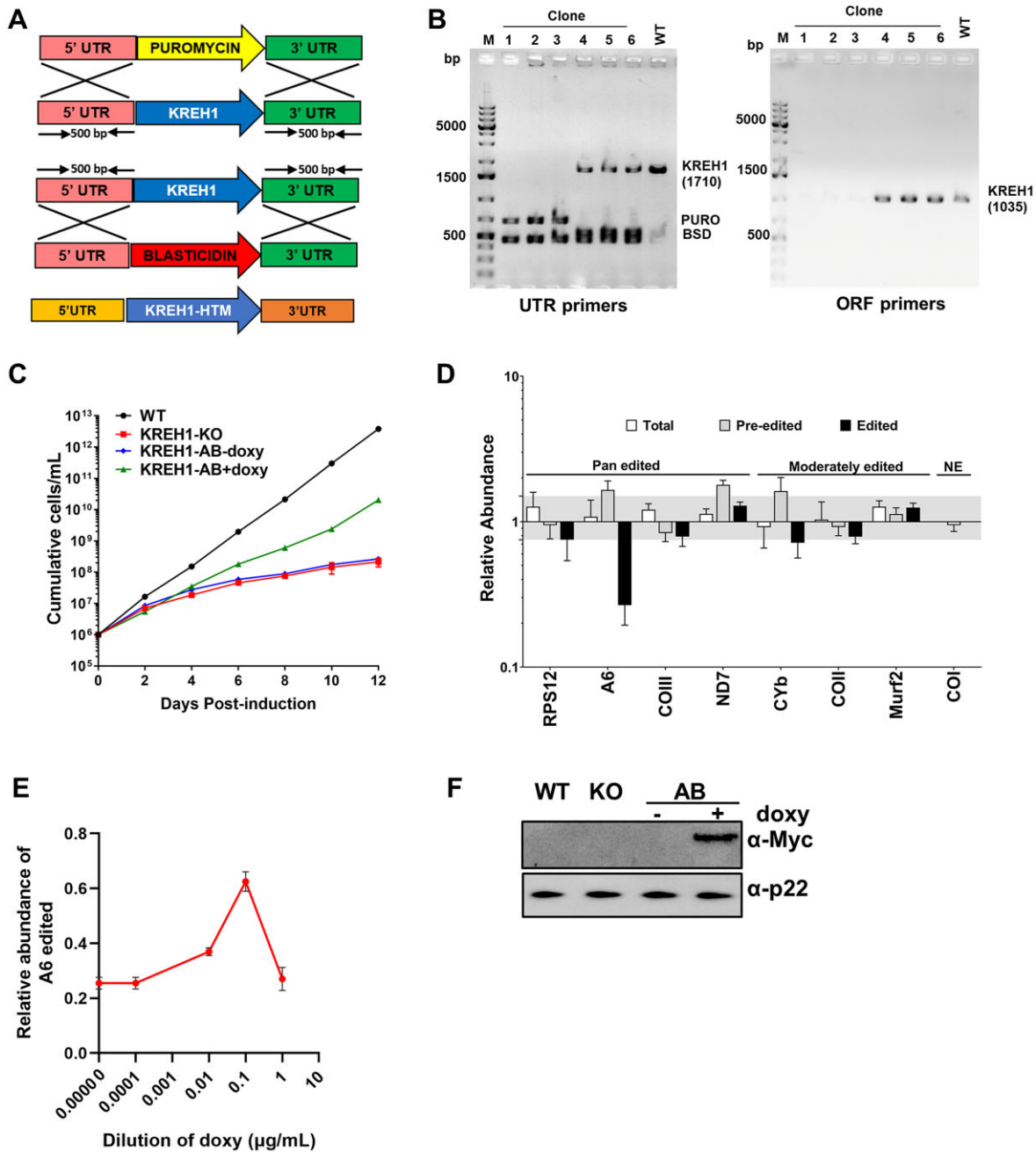


Figure 1. Effects of KREH1 gene disruption on growth and U-indel RNA editing. (A) Schematic representation of the knock out (KO) and add back (AB) strategies. Linearized plasmid was transfected; shown is only the region encompassing and flanking the KREH1 gene and drug resistance markers. (B) KO confirmation by PCR of genomic DNA isolated from six different clones using UTR-based and ORF-based primers. (C) Growth of 29-13 (WT; black), KREH1-KO (red), and KREH1-AB (blue, -doxy; green, +doxy) parasites was monitored for 12 days. Growth rates were examined using one biological replicate each of clones 2 and 3 of KREH1-KO, two replicates of WT, and three replicates of KREH1-AB. (D) RNA was isolated from KREH1-KO and WT *T. brucei* cells and quantified by qRT-PCR using primer sets that specifically detect total, pre-edited, or edited versions of mRNAs. Relative RNA abundance represents RNA levels in KREH1-KO cells compared to levels in WT cells. RNA levels were normalized to 18S rRNA. Levels and numbers represent the mean and standard error of six determinations mRNAs (one biological replicate each of clones 2 and 3, each in technical triplicate). Grey shading indicates 1.5-fold change. (E) Edited A6 mRNA expression in KREH1-AB cells grown in increasing doxycycline concentrations for two days. Abundance is shown relative to that in WT cells. (F) Anti-myc western blot showing expression of KREH1-AB (KREH1-HTM expressed in KREH1-KO cells) after two days growth in 0.1 µg/ml doxycycline. P22 is a loading control.

of 4 $\mu\text{g/ml}$ for 3 days, and KREH1-KO cells (one replicate each of clones 2 and 3) were grown as described above, followed by isolation of RNA using TRIzol per manufacturer's instructions. qRT-PCR was used to validate the level of KREH1 mRNA in KREH1-KO cells, and qRT-PCR and anti-myc western blot were used to validate overexpression levels. cDNA was generated from DNase-treated RNA using gene specific primers described previously (14,18,26,27). These cDNA samples were PCR amplified within the linear range of PCR to maintain the relative abundance of unique fragments. Amplicons were then sequenced using paired-end Illumina MiSeq and paired as described previously (14). The number of total (de-collapsed) and unique (collapsed) reads for each sample are listed in Supplementary Table S2. To normalize the number of reads in each sample, the total (de-collapsed) number of fragments that have no non-T mismatches (standard alignments in Supplementary Table S2) are normalized to 100 000 reads. This normalization scales each sample so that their relative abundance can be compared via their normalized counts (15). TREAT was used as a multiple sequence alignment and visualization tool (14). TREAT consists of a command-line alignment tool along with a built-in web server providing a web-based interface for searching, viewing and analyzing the alignment results. TREAT v0.03 (15) was used in this study. A6 mRNA reads in the two KREH1-KO samples were compared to five wild type (strain 29-13) A6 mRNA samples from a previous study (18). For analysis of KREH1 overexpressor samples, the combined uninduced samples from all three cells lines (6 total) were compared to the two doxycycline-induced biological replicates for each of the three overexpressor cell lines (WT, KA, EQ). Determination of EPSs was performed as described previously (15). The sequencing data used in this study have been deposited in the Sequence Read Archive. A6 mRNA sequences from strain 29-13 were previously published (18) under accession number SRP238943. KREH1-KO and all overexpressor cell line sequences are under accession number SRP346412. KREH1-AB and KREH2 sequences are available under BioProject ID PRJNA936842.

Determination of a junction's pre-edited status in the initiator gRNA region (i.e. quantification of the gRNA skipping phenotype) was done using R. Junction sequences and the pre-edited sequences of A6, RPS12, and CYb mRNAs were imported into RStudio version 1.3.1093. The number of Us at each ES was compared to the expected number of Us at that ES in the pre-edited sequence. Junctions that matched the pre-edited sequence through the entire initiator gRNA region were then identified and quantified. R code used to examine gRNA skipping phenotypes is available on GitHub at <https://github.com/ubccr/treat/tree/master/analysis> and at DOI: 10.5281/zenodo.7795638.

RNA structure predictions were performed with ViennaRNA version 2.4.17 (58). A shortened version of A6 mRNA comprised of editing sites 1–65 was fed into the RNA cofold function along with the alternate initiator gRNA reported by (59). This alternate initiator gRNA was identified as the primary gRNA directing the edited A6 sequences in our lab's *T. brucei* 29-13 population (18). The temperature was set to 27°C for all predictions.

Co-immunoprecipitation and pulldowns

RESC6-PTP, RESC5-MHT and RESC13-10XTY tagged cells harboring KREH1(WT) constructs were grown for 3 days; RESC6-PTP, RESC5-MHT, and RESC13-10XTY tagged cells harboring KREH1(KA) constructs were grown for 2 days in the absence or presence of 4 $\mu\text{g/ml}$ doxycycline. Cells (1×10^{10}) were collected and washed with 1X PBS and Protein A pulldowns of RESC6-PTP were performed as described previously (56). RESC13-10XTY tagged cells were immunoprecipitated using a similar method, except cell lysate was incubated with α -TY antibody pre-bound to Protein A fast flow beads (GE Healthcare). After washing with N150 buffer (50 mM Tris-Cl [pH 7.5], 150 mM NaCl, 0.1% NP-40, 1 mM MgCl_2 and 5 mM β -ME), RESC13 complexes were eluted with 0.1 mM glycine [pH 2.5] followed by neutralization with 1 mM Tris-HCl [pH 8.0]. The levels of target proteins were normalized by western blot before western blotting with specific antibodies against KREPA2 (60), RESC6 (56), RESC13 (31), RESC11A (15), RESC12A (15), RESC14 (26), RESC8 (27) and RESC10 (19).

RNA immunoprecipitation

PF *T. brucei* 29-13, KREH1-WT, and KREH1-KA cells were grown in presence of 4 $\mu\text{g/ml}$ of doxycycline for 2 days. Cells (1×10^{10}) were collected, mitochondria were enriched, and RIP was performed as described previously (19,26,27). Briefly, mitochondrial extracts were immunoprecipitated with α -myc (ICL) beads. Five percent of the beads were taken from each sample, and a western blot was performed to confirm the pulldown of KREH1-Myc proteins. The supernatant was removed after DNaseI (Sigma) treatment followed by proteinase K (Roche) treatment. RNA was extracted with phenol/chloroform followed by ethanol precipitation. RNA was DNase-treated (Ambion DNA-free DNase Kit), and 500 ng of RNA converted to cDNA with *T. brucei* established gene-specific primers targeting either pre-edited or total mRNA (A6, RPS12, CYb, ND8), gA6-1 gRNA or 18S rRNA (18,26) using the iScript cDNA synthesis kit (BioRad). cDNA was amplified using SsoAdvanced PreAmp Supermix (BioRad) and then used for qRT-PCR, with 18S rRNA used for normalization. The $\Delta\Delta\text{Ct}$ method was used to determine the fold change as described previously (26).

RESULTS

KREH1-KO impacts the steady state levels of a subset of mitochondrial transcripts

To understand the mechanism by which KREH1 regulates the U-indel editing process, we generated KREH1-KO cell lines in PF *T. brucei*. KREH1 alleles were sequentially replaced with puromycin (PURO) and blastidicin (BSD) resistance cassettes by homologous recombination (Figure 1A) (54). Incorporation of drug resistance cassettes into the genome and corresponding removal of the KREH1 open reading frame (ORF) was confirmed by PCR analysis of genomic DNA using KREH1 untranslated

region (UTR)-based and ORF-based primers, respectively (Supplementary Table S1). We screened six clones, three of which (clones 1–3) had KREH1 double knock out genotypes (Figure 1B). KREH1-KO cell lines grew significantly slower than wild type (WT) cells, with an approximately 5-fold decrease in doubling time (Figure 1C). To confirm a functional role for KREH1 in RNA editing, we performed qRT-PCR analysis of several mitochondrial transcripts using primers that target total, pre-edited, or edited mRNA (26) (Figure 1D). Similar to previous reports (48,52), we observed decreases in a small subset of edited mRNAs tested in KREH1-KO compared to WT cells. Specifically, *Misael et al.* (52) reported a decrease in edited COII and CYb mRNAs, although pre-edited mRNA also decreased, while *Li et al.* (48) observed significant decreases in A6 and CR3 mRNA editing, with very modest effects on CYb, COII, ND7, COIII and ND9 transcripts. In our panel, we observed a significant editing defect only in A6 mRNA, and this decrease was accompanied by a corresponding increase in pre-edited mRNA. We also observed a very modest effect on CYb mRNA editing. To confirm that the KREH1-KO leads to growth and A6 mRNA editing defects, we generated an add-back (AB) cell line in which we expressed KREH1 with a C-terminal his-TEV-myc (HTM) tag (Figure 1A) (55). Because overexpression of wild type KREH1 itself leads to growth and editing defects (see ahead Figure 4B and C), we titrated KREH1-HTM expression with increasing doxycycline to identify a concentration that restored A6 mRNA editing. We determined that 0.1 $\mu\text{g/ml}$ doxycycline restored edited A6 mRNA to 60% of wild type levels, and thereby established that KREH1-KO is responsible for the editing defect (Figure 1E and F). We next asked if parasite growth was restored by KREH1-AB to a level similar to that of A6 mRNA editing. While uninduced KREH1-AB grew similarly to KREH1-KO, induced KREH1-AB cells demonstrated partial growth restoration as expected (Figure 1C). Collectively, our data confirm that KREH1 is important for cell viability and exerts an effect on the abundance of a subset of fully edited mitochondrial transcripts, with the most significant and reproducible effect across studies being that on A6 mRNA editing.

Single nucleotide level analysis reveals a distinct effect of KREH1 on the earliest stages of editing

Having identified A6 as an mRNA whose editing is substantially impacted by KREH1-KO, we sought to better understand what steps of A6 editing are compromised in the absence of KREH1. To this end, we used Illumina MiSeq sequencing and analysis with the Trypanosome RNA Editing Alignment Tool (TREAT) (14), which allows us to measure proportions of pre-edited, partially edited, and fully edited mRNAs and to analyze partially edited mRNA sequences at the single nucleotide level. Because the edited domain of A6 mRNA is too large to sequence in its entirety using MiSeq, we amplified its 3' edited region using a forward primer that anneals to pre-edited sequence near the middle of the transcript and a reverse primer in the 3' never edited region (see Figure 3A in (18)). With this primer placement, 'fully edited mRNA' described below refers to mRNA intermediates that are fully edited up

to the pre-edited forward primer. Using this analysis, and after normalizing the read counts, we found the proportion of pre-edited reads in KO samples is almost three-fold that of samples isolated from parental 29-13 cells, while the proportion of partially edited reads is concordantly lower (Figure 2A). The KREH1-AB exhibited decreased pre-edited and increased partially edited A6 reads compared to the KREH1-KO (Figure 2A). Fully edited reads are exceedingly rare as seen previously with other pan-edited mRNAs (14–16,19,26,27,61). Thus, in agreement with Figure 1D, the absence of KREH1 results in compromised editing initiation and the accumulation of pre-edited A6 mRNA.

We next determined whether KREH1-KO leads to decreased 3' to 5' editing progression across A6 mRNA as previously reported (48) and, if so, whether pausing occurs at specific positions that could inform KREH1 function. To this end, we determined Exacerbated Pause Sites (EPS) in our KREH1-KO samples relative to parental cell samples as described previously (15) (Table 1 and Supplementary Table S3). Briefly, our TREAT platform defines an ES as any site between two non-U nucleotides in the mRNA sequence numbered starting from the 3' end. Beginning at the 3' end of each unique mRNA read, TREAT then identifies the 5' most ES with continuous correctly edited sequence and designates this site as an Editing Stop Site. EPSs come into play when two RNA populations are compared. Here, any Editing Stop Site for which the number of reads is significantly higher in both replicates of the test condition compared to the number of reads in the control condition is an EPS. A schematic of A6 mRNA sequence, cognate gRNAs, and identified EPSs is shown in Figure 2B. We identified five EPSs in KREH1-KO cells, all within the gRNA-1 and gRNA-2 directed regions, indicating that KREH1 functions in 3' to 5' editing progression, especially across gRNA-1.

Next, we asked whether distinct features of the partially edited population in KREH1-KO cells could illuminate KREH1 function. The sequence 5' of an Editing Stop Site may either be pre-edited or may contain regions of mis-editing at the leading edge of correct editing termed junctions (Table 1). Junctions are commonly thought of as regions of active editing or mis-editing by non-canonical gRNAs, and their sequences in parasites deficient for distinct editing factors can reveal insights into protein function (5,15,19,26,27,62). We also note that TREAT defines junctions as the span between the 5' most editing event and the 3' most mis-edited site in a given mRNA (Table 1); thus, long junctions containing large regions of pre-edited or fully edited sequence are sometimes identified (15,62). We began by analyzing junction lengths in KREH1-KO cells relative to WT cells. We found that KREH1-KO cells have significantly fewer reads with no junction or that contain short junction sequences typical of most edited mRNAs (<20 ES in length) than do WT cells (Figure 3A). Conversely, mRNAs from KREH1-KO cells have a significantly higher frequency of very long junctions (>51 ES in length) (Figure 3A, expanded inset). The increase in very long junctions in KREH1-KO cells suggests that regions of active editing on A6 mRNA are not properly constrained in the absence of this helicase.

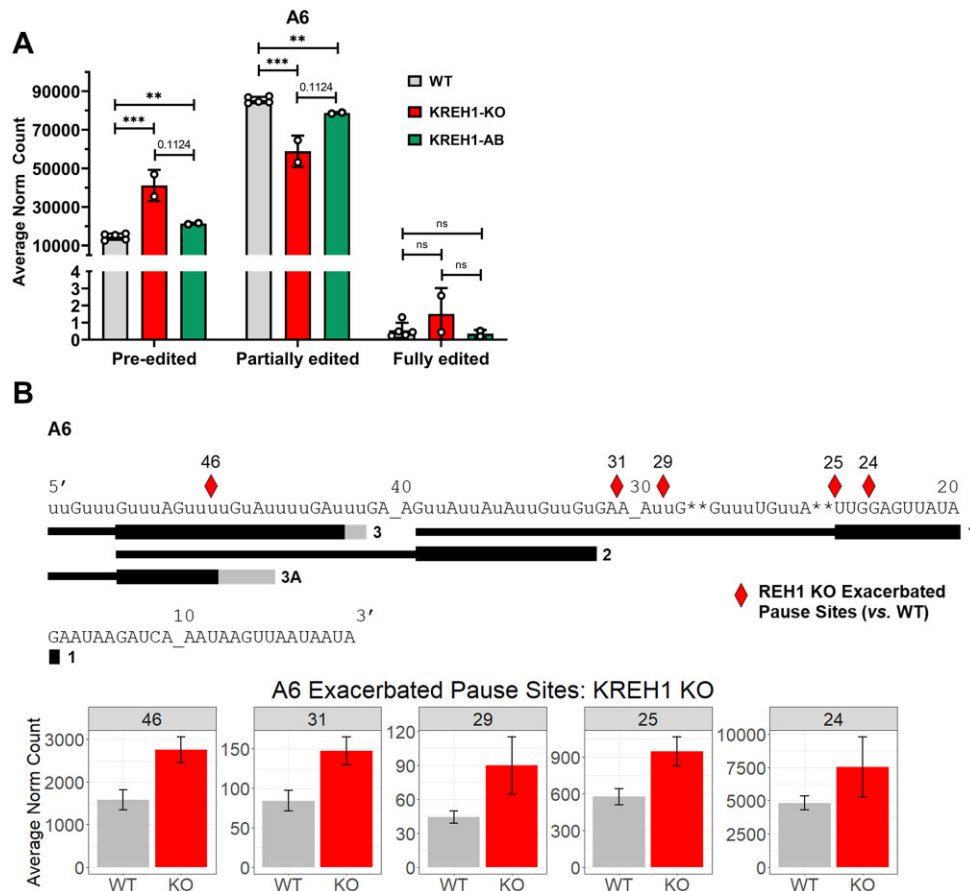


Figure 2. KREH1-KO impacts both editing initiation and progression through the gRNA-1 and gRNA-2 directed blocks of A6 mRNA. (A) Read counts for each sample were normalized to 100 000, and the average levels of normalized pre-edited, partially edited, and fully edited A6 reads were calculated for 29-13 (WT), KREH1-KO, and KREH1-AB samples. Partially edited sequences are defined as reads that are not fully edited but have some U insertion or deletion; fully edited sequences are defined as reads with canonical fully edited sequence up to the 5' primer used for amplification of the A6 mRNA 3' end. (B) Exacerbated Pause Sites (EPSs) were calculated for KREH1-KO samples with WT samples used as the control. Any Editing Stop Site for which the number of reads is significantly higher ($P_{adj} < 0.05$) in the KREH1-KO condition than in the WT for both KO replicates is considered an EPS. Positions of identified EPSs are indicated with red diamonds above fully edited A6 sequence. Numbers indicate ES number. gRNA coverage (59) is shown with black bars; thick black portions represent gRNA anchor sequences. Gray bars represent areas of variable gRNA length. Quantification of the number of reads for each EPS is shown below. Significance was evaluated using Student's *t*-test. ns, not significant; ** $P_{adj} < 0.01$; *** $P_{adj} < 0.001$. Exact padj values are shown for pre-edited and partially edited mRNAs in KREH1-KO versus KREH1-AB in panel A.

Table 1. Definition of terms

| Term (abbreviation) | Definition |
|-------------------------------------|--|
| Editing Site (ES) | Any space between two non-T nucleotides (cDNA) has the potential to be edited at the RNA level and is termed an Editing Site (ES). ES are numbered from 3' to 5' following the direction of editing. |
| Editing Stop Site | Moving 3' to 5', the Editing Stop Site is the final (5' most) ES that matches the canonical fully edited sequence correctly. All ES 3' of the Editing Stop Site match the canonical fully edited sequence. |
| Exacerbated Pause Site (EPS) | An Exacerbated Pause Site is defined as an Editing Stop Site at which the total number of sequences sharing this Editing Stop Site in a sample has increased significantly ($P_{adj} < 0.05$) compared to the uninduced control samples and, thus, is considered a site where editing stalls more in the sample. |
| Junction Start Site (JSS) | The first ES, moving 3' to 5', which does not match the canonical fully edited sequence correctly (can match pre-edited or mis-edited). |
| Junction End Site (JES) | The 5' most ES with any editing action, whether canonical or mis-edited. |
| Junction Length (JL) | The number of ES contained within a junction including both the JSS and JES (e.g. a junction arising after ESS15 with a JES at ES20 would have a JL of 5). |

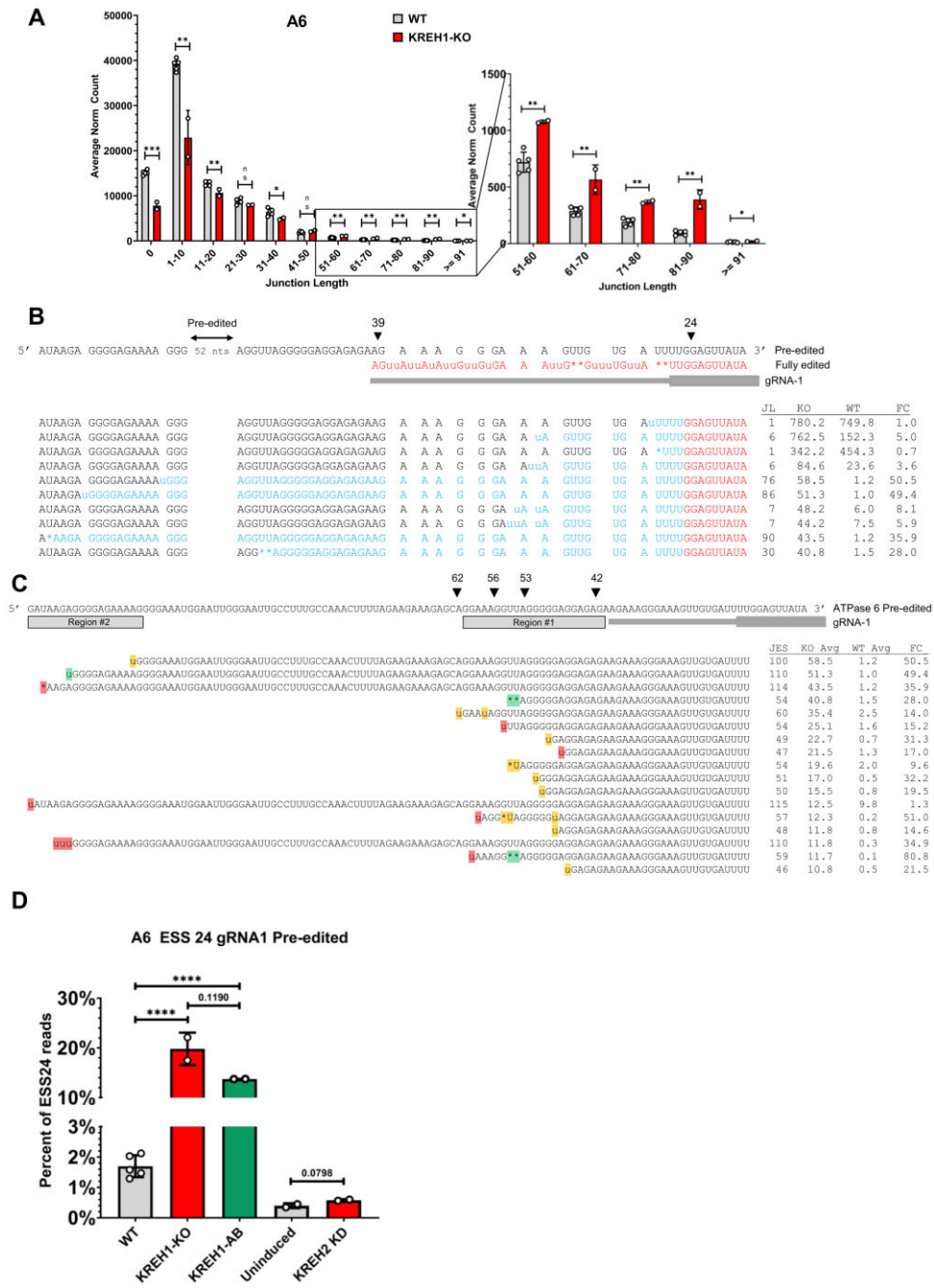


Figure 3. Junction analysis reveals a gRNA skipping phenotype in KREH1-KO. (A) Average number of normalized read counts in different junction length classes for WT and KREH1-KO samples. The length of a junction is the number of ES between the Editing Stop Site and the 5' most ES with any U insertion or deletion. Each Student's *t*-test was performed on *n* = 5 WT and *n* = 2 KREH1-KO samples. ns, not significant; * $P_{adj} < 0.05$; ** $P_{adj} < 0.01$; *** $P_{adj} < 0.001$. (B) The 10 most abundant A6 mRNA sequences with Editing Stop Site 24 in KREH1-KO samples are aligned with pre-edited and fully edited A6 sequences. A 52 nt portion of pre-edited A6 sequence as well as fully edited sequence beyond ES 39 were removed for ease of visualization. The position of the initiator gRNA (gRNA-1) is shown below the fully edited sequence, with the thick portion representing the gRNA anchor region. The junction lengths (JL), averaged normalized counts for KO and WT samples (KO Avg; WT Avg), and fold change (FC) are shown to the right of each sequence. Black text: pre-edited sequence; red text: fully edited sequence; blue text: junction sequence as determined by TREAT. The junction can contain a mixture of pre-edited, fully edited and mis-edited ES. (C) A6 mRNA sequences having Editing Stop Site 24, Junction End Site (JES) > ES39, and pre-edited sequence between ES 24–39 are shown aligned with pre-edited A6 sequence. Only those reads matching this description and present in greater than 10 normalized counts in KREH1-KO samples are shown. Nucleotides 5' of the JES are omitted for clarity. Positions of the initiator gRNA (gRNA-1), Region #1, and Region #2 are indicated by gray bars beneath the A6 pre-edited sequence. ES having undergone an editing action are highlighted according to their accuracy; green: correctly edited site; yellow: incomplete insertion or deletion; red: incorrect insertion or deletion. Arrows pointing to ES 42, 53, 56 and 62 depict the boundaries of predicted unstructured regions shown in Supplementary Figure S2. (D) The proportion of A6 reads with Editing Stop Site 24 and which are pre-edited between ES 25–39 but edited 5' of ES39 was calculated for *n* = 5 WT, *n* = 2 KREH1-KO, *n* = 2 KREH1-AB and *n* = 2 KREH2 knockdown (KD) uninduced and induced samples. Significance was evaluated using Student's *t*-test; **** $P < 0.0001$. Exact *P* values are shown for KREH1-KO versus KREH1-AB and uninduced versus induced KREH2 KD.

To probe the features of the long junctions that accumulate in KREH1-KO cells, we focused our analysis on the EPS at ES24. Because ES24 is the EPS with the largest increase in the number of reads between parental and KREH1-KO samples, defects at this EPS have a larger impact on the overall edited mRNA population than do those at EPS with many fewer reads, such as those at ES25, ES29 and ES31 (Figure 2B). The EPS at ES24 is located immediately preceding the first required editing action, where a deletion of two Us would normally take place at ES25. ES24 is designated as an Editing Stop Site because the 3' anchor region, which is the same sequence in pre-edited and fully edited A6 mRNA, is read by TREAT as a fully edited stretch, and so ES24 is read as the 5' most ES with continuous correctly edited sequence. The higher frequency of reads with Editing Stop Site 24 in our KREH1-KO data indicates that the ability to perform the two U deletion at ES25 is compromised in the absence of KREH1, but that some editing action has taken place. We began by examining the 10 most abundant sequences with Editing Stop Site 24 in our KREH1-KO dataset (Figure 3B). Two of these sequences contain short junctions that do not change in frequency and four sequences increase three- to eight-fold between KREH1-KO and WT samples (Figure 3B, FC). Strikingly, the largest read count increases in KREH1-KO compared to WT samples (28- to 50-fold increase in KREH1-KO samples) occurred in four sequences with long junctions of 30 ES or greater. A close examination of these sequences revealed that they each have one modified ES, and each of these is located outside the range of ESs directed by the initiator gRNA (gRNA-1). To examine the diversity of sequences driving this phenotype in KREH1-KO cells compared to WT, we first searched our data specifically for sequences with Editing Stop Site 24 and with their 5' most editing action 5' of the gRNA-1 directed region, then looked at sequences with at least 10 average normalized counts in KREH1-KO (Figure 3C). The vast majority of these sequences (17/20 or 92.4% of counts) are pre-edited through the region directed by the initiator gRNA (Figure 3C). Similar to the sequences identified in Figure 3B, most are edited at only one ES, with the remainder edited at no more than three ES. Editing actions frequently occur in two distinct regions of the A6 mRNA, labeled 'Region 1' and 'Region 2' (Figure 3C). We also note no clear trend in regard to the accuracy of the editing: some ES are correctly modified according to the eventual canonical edited A6 sequence while others have incomplete or erroneous editing. Based on the absence of editing in the gRNA-1 directed region in these mRNAs, we termed this phenotype 'gRNA skipping'. Overall, 20% of the edited sequences with Editing Stop Site 24 exhibit the gRNA skipping phenotype, a sharp increase from 1.7% in parental cells. The number of such sequences was substantially decreased in the KREH1-AB, from 20% to 13% of sequences with Editing Stop Site 24 (Figure 3D). To further establish the KREH1 specificity of the gRNA skipping phenotype, we tested whether depletion of another editing helicase, KREH2, lead to a similar defect in editing progression. We used high-throughput sequencing (HTS) to analyze A6 mRNA in KREH2 knockdown cells, which have a decrease in edited A6 mRNA similar to that in KREH1-KO by qRT-PCR (Supplementary

Figure S1). We observed no significant increase in gRNA skipping upon KREH2 knockdown, with such sequences constituting <0.6% of Editing Stop Site 24 sequences in either uninduced or induced samples (Figure 3D). These data provide further evidence that the specific function of KREH1 potentiates correct utilization of A6 gRNA-1. We posited there may be some structural basis for the tendency of gRNA skipping to take place in the absence of KREH1. To explore this idea, we generated a structural prediction of the interaction between pre-edited A6 mRNA and the initiator gRNA using ViennaRNA (58). When using a shortened version of A6 as the input mRNA sequence and an initiator gRNA with 15 Us (the number of Us observed in this sequenced gRNA (59)) to evaluate the localized structure of the interaction, ViennaRNA predicted a structure in which the majority of the mRNA region edited via the initiating gRNA is stably duplexed with the gRNA U-tail, while ESs corresponding to Region 1 (roughly ES 42–62) are relatively unstructured (Supplementary Figure S2). Together, our data suggest that KREH1 facilitates localized RNA unwinding to promote productive editing through the A6 gRNA-1 directed region. In the absence of KREH1, editing progression more often pauses within the A6 gRNA-1 directed region or initial editing events take place at regions beyond the initiator gRNA, typically spanning just 1–3 ES.

Expression of helicase-dead KREH1 reveals expanded function in U-indel editing across multiple transcripts

We next used overexpression of WT and helicase-dead KREH1 proteins to further explore KREH1 function in RNA editing. First, we hypothesized that overexpression of dominant negative (DN) mutant proteins might reveal more severe defects in editing compared to those observed by KREH1-KO, similar to previous reports of several DN trypanosome mitochondrial enzymes (34,63,64). Second, by comparing the effects of overexpressing WT and helicase-dead KREH1, we can identify defects specifically dependent on the protein's helicase activity. To this end, we overexpressed WT KREH1 and two mutant derivatives, K168A (KA) and E267Q (EQ), with C terminal HTM tags in *T. brucei*. The mutated K and E residues lie in motifs I and II (DEAD box) of the helicase core, respectively, and both are conserved and essential for helicase function (48,50,51) (Figure 4A). Importantly, the corresponding K to A mutation in KREH1 from *L. tarentolae*, a close *T. brucei* relative, abolished helicase activity *in vitro* (48). Equivalent expression of the three KREH1 derivatives in *T. brucei* was confirmed by α -Myc antibody relative to a p22 control (Figure 4B, D, F; insets) and by qRT-PCR specific for the tagged KREH1 variants (Figure 4C, E, G). Because the overexpressed KREH1 enzymes were recoded for optimal expression, we were unable to amplify endogenous and exogenous enzymes with the same primer sets. Thus, we could not calculate the fold increase in total KREH1 mRNA levels in cells with ectopic KREH1 expression. However, we infer overexpression compared to endogenous levels because the level of endogenous KREH1 mRNA was not changed in cells expressing KREH1-WT or either of the DN mutants (Supplementary Figure S3).

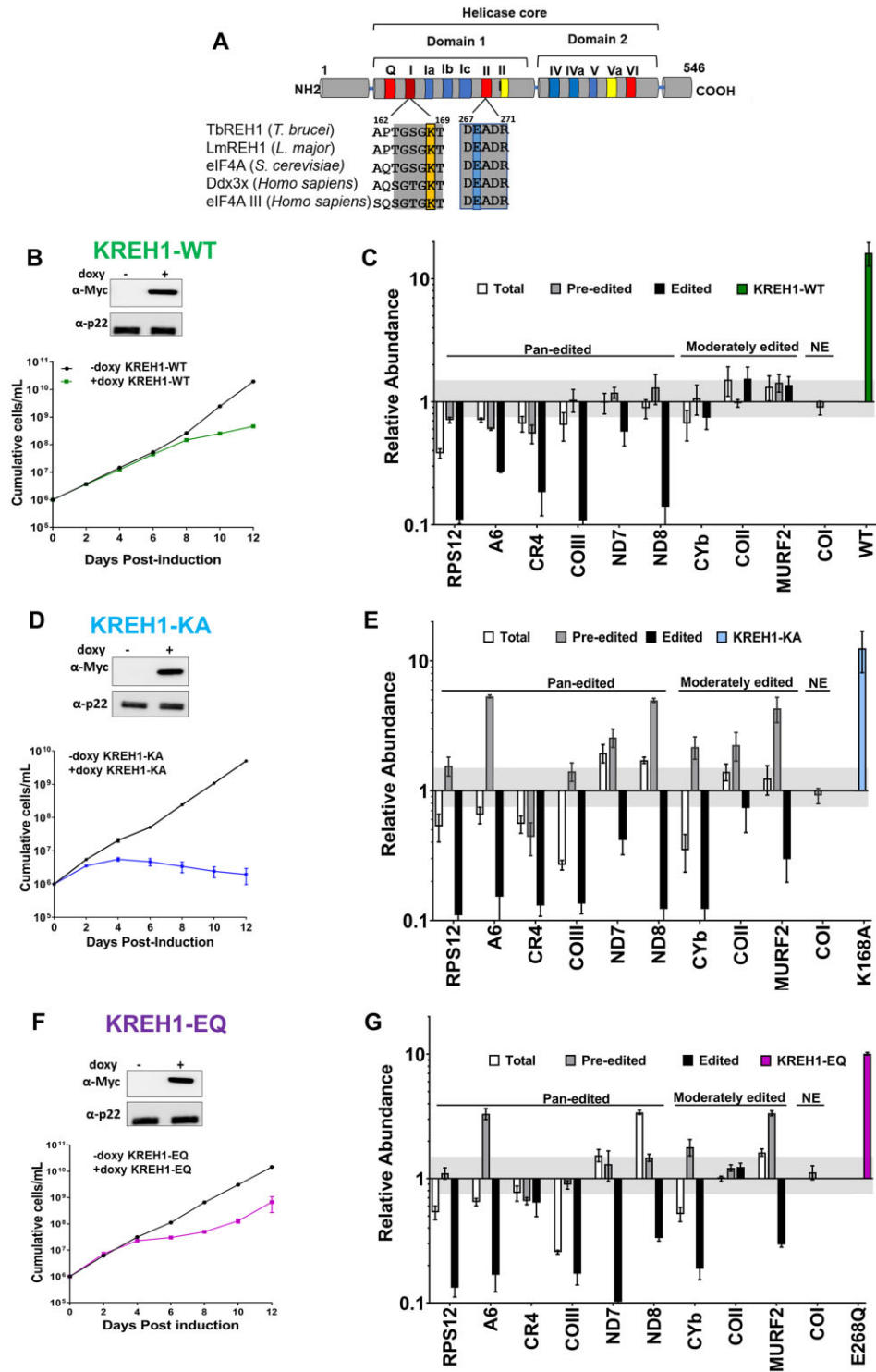


Figure 4. Effect of KREH1-WT, KREH1-KA and KREH1-EQ overexpression on growth and RNA editing. (A) Schematic diagram of DEAD box RNA helicase structure. The DEAD box helicase core consists of two RecA-related domains containing a minimum of 12 conserved motifs that characterize the family. Two motifs, GSGKT and DEAD, are highlighted and demonstrate conservation from trypanosomes to humans. The K and E residues that were mutated are highlighted in yellow and blue, respectively. The figure is not drawn to scale and is adapted from (51). (B, D, F) Growth of triplicate samples of uninduced (-doxy) and induced (+doxy) cells overexpressing KREH1-WT (B), KREH1-KA (D) or KREH1-EQ (F) was monitored for 12 days. Insets: anti-myc western blots showing expression levels of KREH1 variants relative to p22 loading controls. All blots are from the same representative gel, which was cropped for ease of visualization. (C, E, G) Levels of total, pre-edited and edited mRNAs in cells overexpressing KREH1 variants. Levels of mRNAs encoding KREH1 variants are also shown. RNA was isolated from uninduced and induced cells after 3 days of induction and quantified by qRT-PCR. Relative RNA abundance represents RNA levels in induced cells compared to the corresponding uninduced cells. RNA levels were normalized to 18S rRNA, and numbers represent the mean and standard deviation of two biological replicates, each with three technical replicates. Grey shading indicates 1.5-fold change. (C) KREH1-WT; (E) KREH1-KA; (G) KREH1-EQ.

Ectopic expression of KREH1-WT elicited a moderate growth defect beginning on day 8 post-induction, whereas cells overexpressing mutant enzymes displayed earlier and more severe growth defects, with KREH1-KA being most severe (Figure 4B, D and F). Restoration of the growth rate of the KREH1-EQ overexpressor after days 8–10 suggests that these cells escaped doxycycline regulation at this time, potentially due to their inability to tolerate expression of the mutant protein (Figure 4F). qRT-PCR analysis of mitochondrial transcripts from each cell line on day three post-induction revealed significant decreases in multiple edited mRNAs in all lines. However, only KREH1-KA and KREH1-EQ cell lines, and not KREH1-WT, exhibited decreases in editing of the moderately edited CYb and MURF2 and increases in several pre-edited mRNAs (Figure 4C, E, G). Total abundance of some mRNAs was decreased slightly in some cell lines, in particular COIII mRNA in both mutant lines. The abundance of the never edited COI mRNA was unchanged in any overexpressor cell lines. Overall, these results demonstrate that both KREH1-KA and KREH1-EQ mutants exhibit DN phenotypes and reveal KREH1 function in mRNA editing across multiple transcripts. The significantly broader effect of KREH1 DN mutants on RNA editing compared to KREH1-KO (Figure 1D) suggests that other proteins compensate for the loss of KREH1 activity in KREH1-KO. The DN mutants may exert their widespread, and potentially pleiotropic, effects by binding RNA and/or protein partners, but failing to perform their complete functions due to the lack of RNA helicase activity. Together, the effects of overexpression of WT and DN enzymes demonstrate that KREH1 impacts the editing of a wide range of mitochondrial transcripts. The more substantial effect of the DN mutants compared to KREH1-WT suggests that RNA helicase activity is important for the function of KREH1 in mRNA editing.

DN KREH1 overexpression leads to decreased editing initiation

In light of the strong effects of KREH1 DN overexpression on RNA editing observed by qRT-PCR, we further examined the impact of KREH1-KA and KREH1-EQ mutants on editing initiation and progression at the single nucleotide level as described above. We elected to sequence the pan-edited A6 and RPS12 mRNAs from day 3 doxycycline-induced cells due to their similar edited mRNA qPCR profiles between the two mutant expressing cell lines. We also analyzed CYb mRNA as a representative moderately edited transcript. With regard to A6 mRNA, we observed an increase in the proportion of pre-edited reads and a corresponding decrease of partially edited reads in both DN cell lines, but we did not observe similar changes in the KREH1-WT expressing line (Figure 5A). This finding is consistent with the qPCR data indicating a defect in A6 mRNA editing initiation upon KREH1 DN mutant overexpression. To examine potential defects in editing progression, we analyzed EPSs for the KREH1-WT and KREH1 DN samples. We identified eight EPSs in A6 mRNA after KREH1-WT overexpression, three EPSs after KREH1-KA expression, and one EPS after KREH1-EQ overexpression (Figure 5B; Supplementary Figure S4A; Supplementary Table S4). The

eight EPSs detected in the KREH1-WT samples indicate a modest effect on the progression of A6 mRNA editing upon overexpression of the functional helicase. The smaller number of EPSs found in the DN mutant samples compared to KREH1-WT expressing samples and their <2-fold change above uninduced levels (Supplementary Figure S4A; Supplementary Table S4), suggests that A6 mRNA editing in KREH1 DN expressing cells is strongly impacted at the point of editing initiation, with more limited effects on progression.

We next asked if these trends hold true for RPS12 and CYb transcripts. Indeed, TREAT analysis of RPS12 and CYb mRNAs revealed an increase of the proportion of pre-edited reads and a decrease of partially edited reads in KREH1 DN expressing cells relative to uninduced cells (Figure 5C and E). As with A6 mRNA, we also detected fewer EPSs in the KREH1 DN expressing cells than in KREH1-WT expressing cells, with no EPSs identified in CYb mRNA in KREH1 DN overexpressors (Figure 5D and F; Supplementary Figure S4B and C; Supplementary Tables S5 and S6). Unlike what was observed for A6 mRNA, overexpression of KREH1-WT resulted in higher pre-edited RPS12 mRNA levels and lower partially edited RPS12 levels relative to uninduced samples, although the increase in pre-edited mRNAs was not as dramatic in KREH1-WT cells as in the KREH1-DN cells (Figure 5C). The same trend is also observed for CYb mRNA (Figure 5E). Together, single nucleotide level analysis of editing defects in KREH1 overexpressing cells demonstrates that editing initiation is heavily impacted when KREH1 DN mutants are overexpressed, whereas upon WT KREH1-WT overexpression, editing progression is primarily impacted with an additional more modest effect on initiation for some mRNAs. Together, these data are consistent with a model in which KREH1 helicase activity promotes initiation of mRNA editing.

Dominant negative KREH1 overexpression leads to gRNA skipping and initiator gRNA accumulation

Having observed that KREH1-KO results in a substantial increase in the peculiar gRNA skipping phenotype described in this study (Figure 3), we asked whether KREH1 DN overexpression results in an increased number of sequences with the same characteristics. For each of the three mRNAs sequenced, we quantified the number of reads that are pre-edited through the initiator gRNA region (up to ES39 for A6; up to ES22 for RPS12; up to ES569 for CYb) and with some modification further 5'. We found that for each of the three mRNAs, the number of reads displaying gRNA skipping in the initiator gRNA region is significantly increased in cells expressing either the KREH1-KA or KREH1-EQ mutant (Figure 6A–C). In contrast, we observe no such phenotype for KREH1-WT overexpressors in A6 or CYb mRNAs, and only a very small increase in RPS12 mRNA (Figure 6A–C). Thus, similar to the effects of knocking out KREH1, overexpression of KREH1 mutants lacking helicase activity results in a significant impairment of the editing machinery's ability to perform modifications in the mRNA region directed by the initiator gRNA and manifests in a gRNA skipping phenotype.

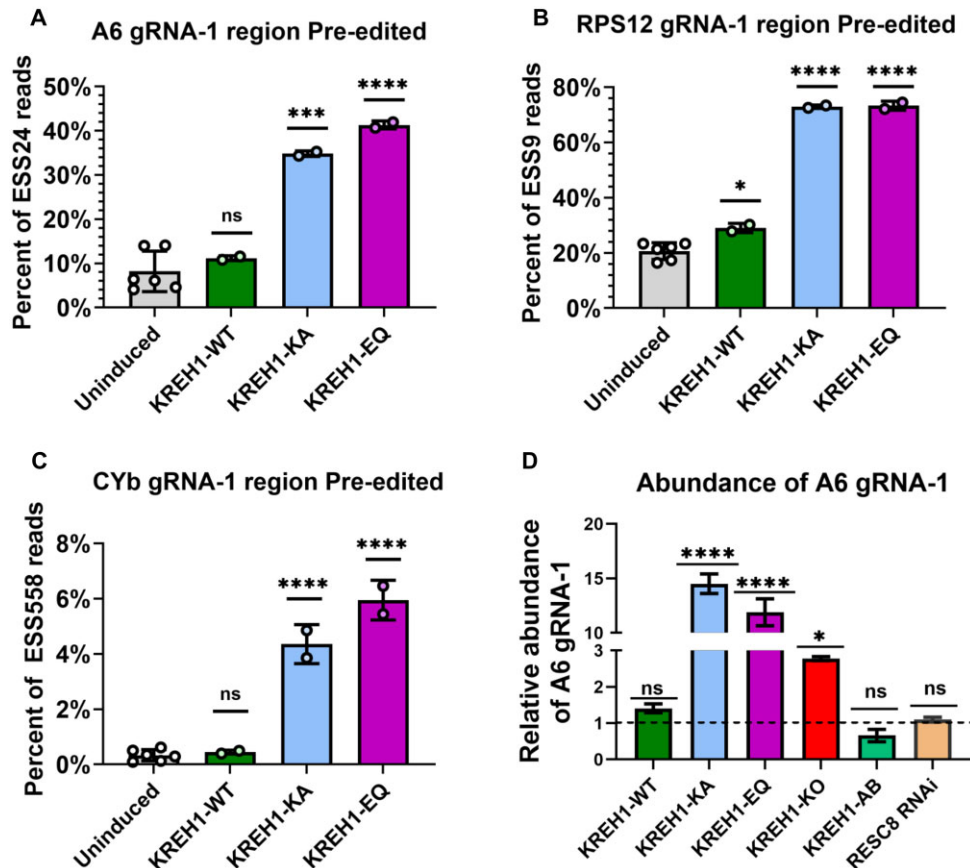


Figure 6. Overexpression of KREH1 dominant negative mutants results in gRNA skipping and initiator gRNA accumulation. Shown in A–C are the proportion of reads for a given mRNA that are pre-edited in the region directed by the first gRNA and contain a modification 5' of this region. (A) The proportion of A6 mRNA reads with Editing Stop Site 24 and which are pre-edited between ES 25–39 and edited 5' of ES39 was calculated for uninduced and induced KREH1 overexpressor samples. (B) Same as in (A), but measuring RPS12 mRNA reads with Editing Stop Site 9 and which are pre-edited between ES 9–22 and edited 5' of ES22. (C) Same as in (A), but measuring CYb reads with Editing Stop Site 558 and which are pre-edited between ES 558–569 and edited 5' of ES569. (D) Abundance of A6 gRNA-1 was measured by qRT-PCR in the induced KREH1 overexpressor lines (plotted relative to the level in the corresponding uninduced cells), in KREH1-KO and KREH1-AB cells (plotted relative to that in WT 29-13 cells), and in induced RESC8 RNAi cells (plotted relative to the corresponding uninduced cells). Dotted line indicates no change compared to control. Student's *t*-tests in (A), (B) and (C) were performed on $n = 6$ combined uninduced samples and $n = 2$ KREH1 OE samples. Student's *t*-tests in (D) were performed on $n = 6$ replicates. ns = not significant; * $P < 0.05$; *** $P < 0.001$; **** $P < 0.0001$.

The occurrence of gRNA skipping across three transcripts in cells expressing DN KREH1 mutants lead us to ask if the abundances of the initiator gRNAs themselves were decreased in DN expressing cell lines compared to the WT expressing lines in which gRNA skipping was not observed. Attempts to amplify initiator gRNAs for RPS12 and CYb mRNAs were unsuccessful; thus, we focused on analysis of A6 gRNA-1 levels. Additionally, because we observed EPSs beyond the A6 gRNA-1 directed region, we also tested whether levels of a non-initiator gRNA (A6 gRNA-2) were affected. Surprisingly, both A6 gRNA-1 and A6 gRNA-2 abundance was higher in both DN mutants compared to the KREH1-WT overexpressing line (Figure 6D and Supplementary Figure S5). To determine if A6 gRNA-1 abundance is always increased parallel to gRNA skipping, we measured A6 gRNA-1 in KREH1-KO and AB cells and observed a 2.5-fold increase in the KO that was ameliorated by the addback of KREH1 (Figure 6D). Finally, to rule out that accumulation of A6 gRNA-1 is a general result of impaired RNA editing, we performed the same

assay on RNA RESC8 knockdown cells, which exhibit both impaired A6 mRNA initiation and progression (27), and observed no A6 gRNA-1 accumulation in these cells (Figure 6D). Together, these data indicate that KREH1 helicase facilitates utilization of initiator, and likely non-initiator, gRNAs across multiple transcripts in a manner that leads to gRNA accumulation.

KREH1-WT and KREH1-KA interact similarly with RNA and the editing machinery

Some DEAD box helicases displace proteins from RNA, act as nucleation centers that establish and stabilize RNPs, or otherwise remodel RNPs in a manner independent of RNA unwinding (51). To ask whether RNP remodeling by KREH1 helicase activity can account for its effects on KREH1 on RNA editing, we first examined whether KREH1-KA and KREH1-WT differ in their protein-RNA and protein-protein interactions. We note that such effects were observed for the KREH2 RNA helicase, in

which the corresponding KA mutant in KREH2 displayed reduced interaction with gRNA, mRNA and a canonical RESC protein compared to the WT enzyme (34). To analyze KREH1 effects, we first performed RNA immunoprecipitation (RIP) analysis of KREH1-WT and KREH1-KA using antibodies against their myc tags and anti-HA antibodies as a negative control (Supplementary Figure S6A). We analyzed both total and pre-edited A6, RPS12, and CYB, mRNAs and the A6 gRNA-1. All transcripts examined, with the exception of total CYB mRNA, were highly enriched in immunoprecipitates of both KREH1-WT and KREH1-KA compared to the mock immunoprecipitation. Comparing KREH1-WT and KREH1-KA enzymes, we observed no difference in the amounts of total A6 mRNA bound and a slight decrease in total RPS12 mRNA. The KREH1-KA mutant did bind more pre-edited mRNA in most cases, which is likely attributable to the increased pre-edited mRNA present in the starting material (compare Figure 4C and E). Thus, mainly the editing status of the bound mRNAs, and not the total amount of mRNA, differed between KREH1-WT and KREH1-KA, consistent with the DN effect of KREH1-KA expression on editing initiation. We also observed a slight increase in A6 gRNA-1 association with KREH1-KA, which may be partially due to increased total levels of this gRNA (see Figure 6D). Overall, since differences in RNA binding between KREH1-KA and KREH1-WT primarily reflect differences in the input, we conclude that the distinct editing phenotypes between KREH1-WT and KREH1-KA are unlikely to be due to dramatic differences in their RNA binding.

We next asked whether the differences in the editing phenotypes between KREH1-WT and KREH1-KA are correlated with a difference in the association of these enzymes with distinct components of the editing holoenzyme. Previous studies reported interactions between KREH1 and some RECC and RESC components (35,43–47). Here, we monitored several RESC components as these proteins may act differently due to the heterogeneous and dynamic nature of RESC (Supplementary Figure S6B). In contrast, RECC is a more stable complex, and we thus only monitored its KREPA2 component. After confirming that the steady state levels of these factors are unchanged upon overexpression of KREH1-WT or KREH1-KA (Supplementary Figure S7), we performed co-immunoprecipitation assays with the KREH1-WT and DN mutant proteins. Both KREH1-WT and KREH1-KA interact with RESC (RESC13, RESC2, RESC6 and RESC8) as well as RECC (KREPA2), and we did not observe any differences between the KREH1-WT and KREH1-KA enzymes with these holoenzyme components (Supplementary Figure S6C and D). Overall, from the above results we conclude that KREH1-WT and KREH1-KA interact with components of RESC and RECC to the same extent, and helicase activity does not affect these interactions.

Overexpression of both KREH1-WT and KREH1-KA disorders holoenzyme homeostasis

We next asked whether overexpression of KREH1-WT and the DN KREH1 differentially affects RNA editing holo-

zyme homeostasis. RECC interacts transiently with RNA bound RESC complexes (Supplementary Figure S6B), and KREH1 interacts transiently or sub-stoichiometrically with both RECC and RESC (3,46). Hence, one can envision that if KREH1 exhibits RNP remodeling activity, its association with the editing holoenzyme might alter holoenzyme interactions or composition, and disruption of this activity in DN mutants could lead to editing defects. To determine how overexpression of KREH1 affects the integrity of RESC as well as RESC-RECC complexes, and whether WT and DN mutant proteins exhibit different phenotypes, we generated several cell lines harboring doxycycline regulatable KREH1-WT or KREH1-KA overexpression and constitutively tagged versions of either RESC13-10xTY (REMC module of RESC), RESC6-PTP (GRBC module of RESC) and KREPB5-MHT (RECC). We then analyzed the effects of KREH1-WT and KREH1-KA overexpression on distinct intra-RESC as well as RESC-RECC interactions by co-precipitation. When RESC6-PTP was precipitated in the presence and absence of overexpressed KREH1-WT, we observed that many RESC components tested (REMC module proteins RESC11A, RESC12A, RESC13, and organizer proteins RESC10 and RESC14) showed decreased association with RESC6 when KREH1-WT is overexpressed. The exceptions were RESC2 and RESC8, which showed unchanged or slightly increased interactions with RESC6, respectively (Figure 7A and C). Cells overexpressing KREH1-KA exhibited a similar phenotype as KREH1-WT overexpressors, except that the RESC6-RESC8 interaction was disrupted in the DN mutant overexpressor (Figure 7B and D). To further probe the effects of KREH1 overexpression on holoenzyme homeostasis, we immunoprecipitated RESC13-10xTY in the presence and absence of KREH1-WT. Interactions between RESC13 and its known partners, RESC11A and RESC12A, were essentially unaffected by KREH1-WT overexpression, as was the RESC13-RESC2 interaction (Figure 7E and G). In contrast, RESC13 interactions with GRBC module protein RESC6 and organizer proteins RESC10 and RESC14 were decreased when KREH1-WT was overexpressed (Figure 7E and G). Interestingly, as observed with RESC6 (Figure 7A and C), RESC13 association with RESC8 was slightly increased by KREH1-WT OE (Figure 7E and G). When we examined the effect of overexpressing the KREH1-KA mutant in the RESC13-10xTY background, again REMC interactions remained strong, but in this case all other components tested exhibited decreased interactions (Figure 7F and H). To probe RESC-RECC interactions in KREH1-WT and KREH1-KA overexpressing cells, we precipitated the RECC component, KREPB5, and tested for interactions of several RESC components (Figure 8). Interestingly, we were not able to detect associations between KREPB5 and RESC6, RESC8, or RESC10. We detected disruption of essentially all identifiable RECC-RESC interactions in both cell lines, with the exception of the RESC2 interaction in KREH1-KA cells. In summary, while a few editing holoenzyme protein-protein interactions differed between cells overexpressing KREH1-WT and KREH1-KA, both cell lines displayed significantly disrupted intra-RESC and RESC-RECC interactions. Thus, we conclude that KREH1-KA specific alterations to holoenzyme

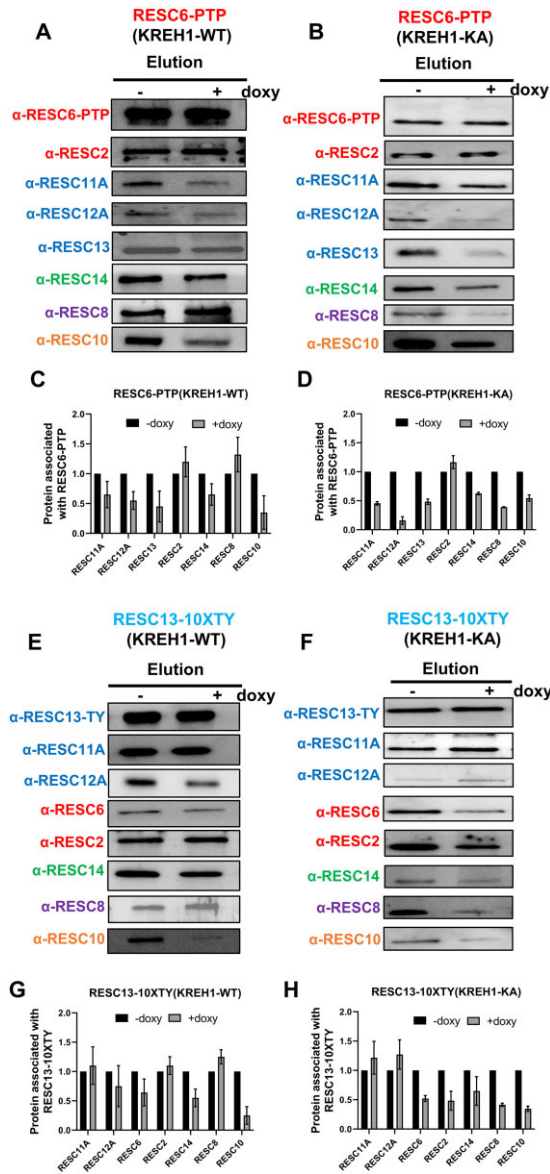


Figure 7. Effect of overexpression of KREH1-WT and KREH1-KA on intra-RESC protein–protein interactions. (A) Precipitation of RESC6-PTP was performed from lysates of KREH1-WT overexpressing cells either uninduced (–doxy) or induced (+doxy) after a 3-day induction. Bound proteins were released by TEV cleavage, and RESC6 was normalized in the elutions by western blot. Normalized elutions were analyzed by western blot with antibodies against RESC components. (B) As in A, but with lysates from KREH1-KA overexpressing cells. (C) Quantification of (A). Levels in –doxy samples were set to 1.0. Bar graphs represent the average and standard deviation of two biological replicates each with two technical replicates. (D) Quantification of (B). Levels in –doxy samples were set to 1.0. Bar graphs represent the average and standard deviation of two biological replicates each with two technical replicates. (E) IP of RESC13-10XTY was performed from lysates of KREH1-WT uninduced (–doxy) and induced (+doxy) cells as in A. Bound proteins were released by 100 mM glycine (pH 2.5), and RESC13 was normalized in the elutions by western blot. Normalized elutions were analyzed by western blot with antibodies against RESC components. (F) As in E, but with lysates from KREH1-KA overexpressing cells. (G) Quantification of (E). Levels in –doxy samples were set to 1.0. Bar graphs represent the average and standard deviation of two biological replicates each with two technical replicates. (H) Quantification of (F). Levels in –doxy samples were set to 1.0. Bar graphs represent the average and standard deviation of two biological replicates each with two technical replicates.

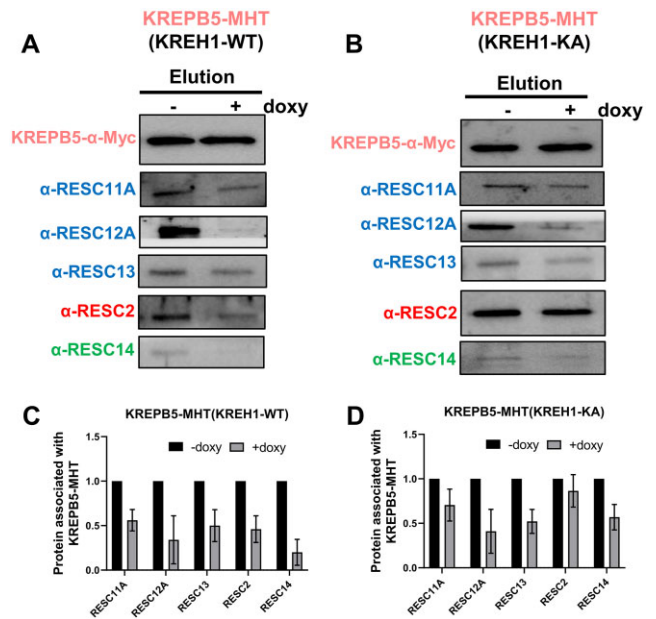


Figure 8. Effect of overexpression of KREH1-WT and KREH1-KA on RECC-RESC protein–protein interactions. (A) Precipitation of KREP5-MHT was performed from lysates of KREH1-WT uninduced (–doxy) and induced (+doxy) cells, after a 3 day induction. Bound proteins were released by TEV cleavage, and KREP5-Myc was normalized in the elutions by western blot. Normalized elutions were analyzed by western blot with antibodies against RESC components. (B) As in A, but using lysates of KREH1-KA cells. (C) Quantification of (A). Levels in –doxy samples were set to 1.0. Bar graphs represent the average and standard deviation of two biological replicates each with two technical replicates. (D) Quantification of (B). Levels in –doxy samples were set to 1.0. Bar graphs represent the average and standard deviation of two biological replicates each with two technical replicates.

homeostasis are unlikely to account for the striking disruptions to U-indel editing observed in these DN mutant KREH1 expressing cells compared to those overexpressing KREH1-WT.

DISCUSSION

DEAD box RNA helicases play important roles in almost all aspects of RNA biology in all three domains of life, using ATP to remodel RNA and RNP complexes (50,51,65). For example, eight RNA helicases drive the extensive conformational and compositional rearrangements of the spliceosome during the splicing cycle, with four involved in assembly and activation and four critical for catalysis and disassembly. Five additional helicases function in splicing in metazoans. The Dbp5 DEAD box helicase is primarily localized at the cytoplasmic rim of nuclear pores, where its interaction with Gle1 and inositol hexakisphosphate are thought to stimulate the release of Mex67 and Nab2 from mRNA to facilitate nuclear mRNA export. Finally, eIF4A is an abundant DEAD box helicase that is critical in the formation of a translation initiation complex that allows the small ribosomal subunit to bind to mRNA during cytoplasmic translation. The complexity of mRNA editing in kinetoplastid mitochondria rivals that of pre-mRNA splicing and translation, entailing the dynamic interaction of

the multi-protein and modular RECC and RESC complexes, and numerous accessory factors (3). Editing also involves extensive RNA-RNA interactions, with most mRNAs requiring the sequential and ordered action of dozens of *trans*-acting gRNAs for generation of a completely edited mRNA. Given this scenario, it is not surprising that three RNA helicases are reportedly associated with the editing holoenzyme: KREH1, KREH2 and KREH3.

The aim of this study was to determine the function of the KREH1 DEAD box RNA helicase in U-indel editing in kinetoplastid protozoa. Using KREH1-KO and DN mutant expressing cell lines and a combination of HTS and biochemical approaches, we show that KREH1 interacts with the editing machinery and its RNA substrates, and that its helicase activity impacts the editing of a broad range of mitochondrial mRNAs. Specifically, we observed substantially decreased editing initiation as well as the presence of a distinct impairment of editing progression in A6 mRNA upon KREH1-KO and across multiple mRNAs in KREH1 DN expressing cells. The latter phenotype, termed gRNA skipping, is characterized by a complete bypass of the mRNA region whose editing is directed by the initiating gRNA and the occurrence of one or a few editing events 5' of this region. gRNA-mRNA modeling, although only theoretical, suggests that extensive basepairing between A6 gRNA-1 and pre-edited mRNA sequences may render the 3' most region of A6 mRNA inaccessible to the editing machinery in the absence of KREH1 activity. We also observed a few distinct pauses in editing progression across the gRNA-1 and gRNA-2 directed regions of A6 mRNA upon KREH1-KO. Surprisingly, we did not detect any EPS at the ends of gRNAs upon KREH1-KO, which would be expected if KREH1 functions in gRNA removal, as previously hypothesized (48). However, we cannot rule out that substantial 3' initiation and progression defects masked such an effect in our system. Co-precipitation and RIP analyses failed to identify dramatic differences between KREH1-WT and DN KREH1 with respect to editing machinery interactions or homeostasis, ruling out major contributions of perturbed macromolecular interactions to the initiation and gRNA skipping phenotypes observed in cells overexpressing DN KREH1. Thus, our data support a model in which KREH1 RNA helicase activity remodels the gRNA-mRNA duplex to permit accurate utilization of the initiating gRNA (Figure 9).

Single nucleotide analysis of mRNAs from cells overexpressing KREH1-WT indicate that, in addition to KREH1's impact on editing initiation and initiator gRNA utilization, this helicase likely impacts editing along the entire length of a given mRNA. In KREH1-WT overexpressing cells, we observed numerous EPSs throughout the A6 and RPS12 mRNAs, into the regions edited by the fifth and eleventh gRNAs, respectively. We envision that, in these cases, excess KREH1-WT interacts with multiple gRNA-mRNA duplexes across an mRNA and promiscuously remodels them in an unproductive manner. Previous structure probing experiments showed that four different gRNAs, including A6 gRNA-1, form similar structures comprising two imperfect stemloops (66). Thus, gRNA and gRNA-mRNA structural features may be relatively consistent across the length of a given mRNA, and these el-

ements presumably need to be remodelled for complete gRNA utilization. Together, these observations suggest that the role of KREH1 in remodeling initiator gRNA-mRNA duplexes described herein is likely also important for numerous more 5' gRNA-mRNA structures. Additionally, because those mRNAs that exhibit gRNA skipping appear to have undergone one to three gRNA-independent editing events, it is possible that KREH1 also promiscuously remodels mRNA duplexes, which then preferentially interact with and are utilized by the editing machinery. It was previously demonstrated that KREH1 interacts with RECC, and that these interactions take place through an RNA linker (44,48). More recently, biotin ligase assays with several RESC proteins (RESC2, RESC5, RESC7 and RESC13) showed that KREH1 is in-network with these RESC components along with KPAF4, which is the part of polyadenylation complex (46). Our immunoprecipitation results confirmed the interaction of KREH1 with RECC, as well as with the GRBC (Guide RNA Binding Complex) and REMC (RNA Editing Mediator Complex) modules and organizer proteins of RESC. RIPs demonstrated that KREH1 interacts with both mRNA and gRNA. Moreover, overexpression of DN KREH1 lead to accumulation of both A6 gRNA-1 and A6 gRNA-2. The broad association of KREH1 with the editing and polyadenylation machineries and both mRNA and gRNA, the effects of KREH1-WT overexpression on editing progression, and effects of DN KREH1 expression on both initiator and non-initiator gRNAs are consistent with KREH1 function during both editing initiation and progression across multiple gRNA-directed editing blocks throughout the length of the mRNA.

Our finding that overexpression of enzyme-dead KREH1 mutants leads to a much broader effect on U-indel editing than does KREH1-KO indicates that other factors can compensate for KREH1 in its absence, and these factors are partially redundant with KREH1 in WT cells. Two DEAH/RHA family RNA helicases, KREH2 and KREH3, reportedly associate with components of the editing holoenzyme (4,47,49). KREH2, which also interacts with KREH1 in RNase-treated 20–30S glycerol gradient fractions (47), has been well studied. Overexpression of KREH2 results in a similar phenotype as KREH1 overexpression in that both WT and helicase-dead KREH2 mutants impact growth, with mutants having a more deleterious effect (47). However, KREH2 appears to be the dominant helicase involved in U-indel editing as RNAi-mediated depletion of KREH2 causes decreased levels of most edited mRNAs (28,34). KREH2 knockdown affects the majority of editing blocks across several pan-edited mRNAs, and impacts the editing of RESC-associated mRNAs (16,34), although KREH2 appears to have a limited effect on editing initiation, as its depletion does not cause significant increases in most pre-edited mRNAs (28). KREH3 knockdown reportedly does not affect the levels of edited mRNAs (34), although neither knock out nor dominant negative studies of this enzyme have been performed. A dual knockdown of KREH1 and KREH3 may be informative regarding potential redundant functions. Together, current data suggest a model in which KREH2 has a broad substrate range, while KREH1 (and possibly KREH3) exhibits

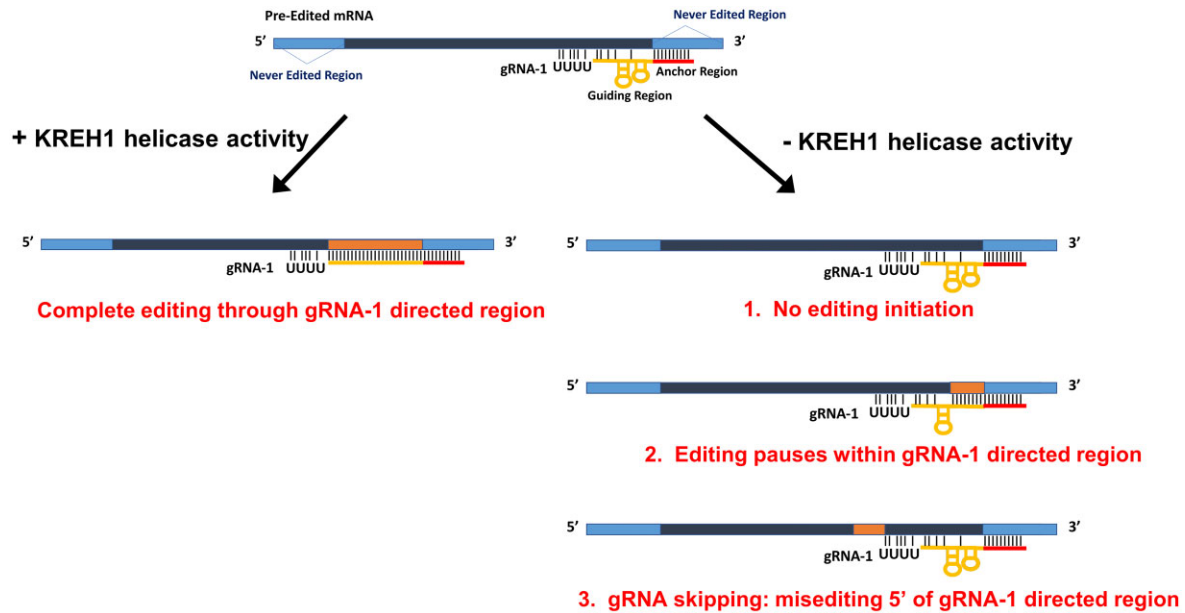


Figure 9. Model of KREH1 function during utilization of initiator gRNAs. See text for details. Blue, never edited sequence; orange, edited sequence; black, pre-edited sequence; red, gRNA anchor region; yellow, gRNA guiding region.

more specific activity towards a distinct subset of gRNA-mRNA structures. KREH2's relaxed specificity then allows it to sufficiently remodel typical KREH1 RNA structures when KREH1 is missing to allow full editing of most mRNAs. In addition to RNA helicases, we cannot rule out that some RESC proteins participate in RNA remodeling in a manner redundant with KREH1, as the majority of RESC proteins have RNA binding activity, and RESC13 also promotes RNA annealing (15,17,19,27–29,31,32). Indeed, a small proportion of mRNAs in RESC13 and RESC12A knockdowns showed disjointed editing features reminiscent of, but not identical to, the gRNA skipping phenotype (15). In these cases, the disjointed edited region was much further 5' than that observed in KREH1-KO cells. But again, in the absence of KREH1, these proteins may be able to exert their activities on KREH1 substrates. Finally, 20S complexes primarily composed of RECC proteins reportedly execute RNA unwinding activity (67). Thus, it appears that the editing machinery contains multiple RNA remodeling components that can, to some extent, compensate for each other.

Our analysis of editing holoenzyme interactions in KREH1-WT and KREH1-KA cells contributes to further understanding of the editing machinery. Pulldown of RECC revealed its strong association with only a subset of RESC components. We readily detected interactions between RECC and RESC11A, RESC12A, and RESC13, which are components of the REMC module, as well as the gRNA binding RESC2 and organizer RESC14 in both KREH1-WT and KREH1-KA cell lines. In general, little difference was observed between WT and mutant, with the exception that the KREH1-KA mutant exhibited slightly increased interactions with RESC2 compared to KREH1-WT. Strikingly, while we detected RECC association with the REMC module of RESC, we were unable to detect

RECC interactions in either cell line with the GRBC module protein, RESC6, or the organizers, RESC8 or RESC10. These data are in line with the mass spectrometry studies performed by Aphasizheva *et al.* (35), which suggested that REMC bridges RECC and GRBC. On the other hand, while the previous authors included RESC8 in the REMC module, our inability to detect a RECC-RESC8 interaction suggests that RESC8 is not a dedicated REMC protein. Rather, these data support our previously published model in which RESC8 acts as a scaffold that promotes and modulates RESC-GRBC interactions, but whose continued interaction with the assembled complex is not required (27). Interestingly, we also found that overexpression of KREH1-WT promoted, in *trans*, the interactions between RESC8 and both GRBC (RESC6) and REMC (RESC13), whereas KREH1-KA expression diminished these interactions (compare Figure 7C and D and G and H). Indeed, the RESC8 interactions with both RESC modules are modestly increased in KREH1-WT overexpressing cells compared to uninduced parental cells. Thus, KREH1 may alter RNA structure in such a way that increases its recognition by RESC8, which is an RNA binding protein. Alternatively, KREH1-mediated alterations in RNA structure may preclude normal RESC8 release from assembled RESC, thereby inhibiting necessary dynamic RESC changes and causing the abundant editing pauses across mRNAs that we observed when KREH1-WT is overexpressed.

In summary, our combined transcriptomic and biochemical data support a broad function for the KREH1 helicase in U-indel RNA editing. Future experiments entailing iCLIP analysis of KREH1 RNA binding sites, as well as genetic experiments to discern the functional interplay between mitochondrial helicases will be important future directions for expanding our understanding of KREH1's role in U-indel RNA editing.

DATA AVAILABILITY

RNAseq data are available at the Sequence Read Archive under accession numbers SRP238943 (A6 mRNA sequences from strain 29-13) and SRP346412 (all sequences from KREH1-KO and overexpression cell lines). KREH1-AB and KREH2 sequences are available under BioProject ID PRJNA936842. R code used to determination a junction's pre-edited status in the initiator gRNA region (*i.e.* quantification of the gRNA skipping phenotype) can be found at DOI: 10.5281/zenodo.7795638.

SUPPLEMENTARY DATA

Supplementary Data are available at NAR Online.

ACKNOWLEDGEMENTS

We thank Ken Stuart for antibodies against KREPA2 and Joseph Smith for critical reading of the manuscript. We gratefully acknowledge the support of the University at Buffalo Genomics and Bioinformatics Core, especially Jonathan Bard, and the University at Buffalo Center for Computational Research, especially Andrew Bruno. We also thank Bri Cunneen for technical support.

FUNDING

National Institutes of Health [R21 AI131448, R01 GM129041 to L.K.R.]; National Institutes of Health [R01 RCA241123 to Y.S.]; UB Mark Diamond Research Fund to K.S.]. Funding for open access charge: National Institutes of Health [R01 GM129041].

Conflict of interest statement. None declared.

REFERENCES

- Maslov,D.A., Opperdoes,F.R., Kostygov,A.Y., Hashimi,H., Lukeš,J. and Yurchenko,V. (2019) Recent advances in trypanosomatid research: genome organization, expression, metabolism, taxonomy and evolution. *Parasitology*, **146**, 1–27.
- Butenko,A., Hammond,M., Field,M.C., Ginger,M.L., Yurchenko,V. and Lukeš,J. (2021) Reductionist pathways for parasitism in euglenozoans? Expanded datasets provide new insights. *Trends Parasitol.*, **37**, 100–116.
- Aphasizheva,I., Alfonso,J., Carnes,J., Cestari,I., Cruz-Reyes,J., Goringe,H.U., Hajduk,S., Lukes,J., Madison-Antenucci,S., Maslov,D.A. *et al.* (2020) Lexis and grammar of mitochondrial RNA processing in trypanosomes. *Trends Parasitol.*, **36**, 337–355.
- Cruz-Reyes,J., Mooers,B.H., Doharey,P.K., Meehan,J. and Gulati,S. (2018) Dynamic RNA holo-editosomes with subcomplex variants: insights into the control of trypanosome editing. *Wiley Interdiscip. Rev. RNA*, **9**, e1502.
- Zimmer,S.L., Simpson,R.M. and Read,L.K. (2018) High throughput sequencing revolution reveals conserved fundamentals of U-inde editing. *Wiley Interdiscip. Rev. RNA*, **9**, e1487.
- Read,L.K., Lukeš,J. and Hashimi,H. (2016) Trypanosome RNA editing: the complexity of getting U in and taking U out. *Wiley Interdiscip. Rev. RNA*, **7**, 33–51.
- Schnauffer,A., Panigrahi,A.K., Panicucci,B., Igo,R.P., Salavati,R. and Stuart,K. (2001) An RNA ligase essential for RNA editing and survival of the bloodstream form of *Trypanosoma brucei*. *Science*, **291**, 2159–2162.
- Salavati,R., Ernst,N.L., O'Rear,J., Gilliam,T., Tarun,S. Jr and Stuart,K. (2006) KREPA4, an RNA binding protein essential for editosome integrity and survival of *Trypanosoma brucei*. *RNA*, **12**, 819–831.
- Koslowsky,D.J., Bhat,G.J., Perrollaz,A.L., Feagin,J.E. and Stuart,K. (1990) The MURF3 gene of *T. brucei* contains multiple domains of extensive editing and is homologous to a subunit of NADH dehydrogenase. *Cell*, **62**, 901–911.
- Feagin,J.E., Abraham,J.M. and Stuart,K. (1988) Extensive editing of the cytochrome c oxidase III transcript in *Trypanosoma brucei*. *Cell*, **53**, 413–422.
- Benne,R., Van Den Burg,J., Brakenhoff,J.P., Sloof,P., Van Boom,J.H. and Tromp,M.C. (1986) Major transcript of the frameshifted coxII gene from trypanosome mitochondria contains four nucleotides that are not encoded in the DNA. *Cell*, **46**, 819–826.
- Blum,B., Bakalara,N. and Simpson,L. (1990) A model for RNA editing in kinetoplastid mitochondria: “guide” RNA molecules transcribed from maxicircle DNA provide the edited information. *Cell*, **60**, 189–198.
- Seiwert,S.D. and Stuart,K. (1994) RNA editing: transfer of genetic information from gRNA to precursor mRNA *in vitro*. *Science*, **266**, 114–117.
- Simpson,R.M., Bruno,A.E., Bard,J.E. and Buck,M.J. (2016) High-throughput sequencing of partially edited trypanosome mRNAs reveals barriers to editing progression and evidence for alternative editing. *RNA*, **22**, 677–695.
- Simpson,R.M., Bruno,A.E., Chen,R., Lott,K., Tylec,B.L., Bard,J.E., Sun,Y., Buck,M.J. and Read,L.K. (2017) Trypanosome RNA editing mediator complex proteins have distinct functions in gRNA utilization. *Nucleic Acids Res.*, **45**, 7965–7983.
- Kumar,V., Ivens,A., Goodall,Z., Meehan,J., Doharey,P.K., Hillhouse,A., Hurtado,D.O., Cai,J.J., Zhang,X., Schnauffer,A. *et al.* (2020) Site-specific and substrate-specific control of accurate mRNA editing by a helicase complex in trypanosomes. *RNA*, **26**, 1862–1881.
- Dixit,S., Müller-McNicoll,M., David,V., Zarnack,K., Ule,J., Hashimi,H. and Lukeš,J. (2017) Differential binding of mitochondrial transcripts by MRB8170 and MRB4160 regulates distinct editing fates of mitochondrial mRNA in trypanosomes. *Mbio*, **8**, e02288-16.
- Smith,J.T. Jr, Doleželová,E., Tylec,B., Bard,J.E., Chen,R., Sun,Y., Ziková,A. and Read,L.K. (2020) Developmental regulation of edited cyb and COIII mitochondrial mRNAs is achieved by distinct mechanisms in *Trypanosoma brucei*. *Nucleic Acids Res.*, **48**, 8704–8723.
- Dubey,A.P., Tylec,B.L., McAdams,N.M., Sortino,K. and Read,L.K. (2021) Trypanosome RNA editing substrate binding complex integrity and function depends on the upstream action of RESC10. *Nucleic Acids Res.*, **49**, 3557–3572.
- Tylec,B.L., Simpson,R.M., Kirby,L.E., Chen,R., Sun,Y., Koslowsky,D.J. and Read,L.K. (2019) Intrinsic and regulated properties of minimally edited trypanosome mRNAs. *Nucleic Acids Res.*, **47**, 3640–3657.
- Gerasimov,E.S., Gasparyan,A.A., Afonin,D.A., Zimmer,S.L., Kraeva,N., Lukeš,J., Yurchenko,V. and Kolesnikov,A. (2021) Complete minicircle genome of *Leptomonas pyrrochoris* reveals sources of its non-canonical mitochondrial RNA editing events. *Nucleic Acids Res.*, **49**, 3354–3370.
- Koslowsky,D.J., Bhat,G.J., Read,L.K. and Stuart,K. (1991) Cycles of progressive realignment of gRNA with mRNA in RNA editing. *Cell*, **67**, 537–546.
- Carnes,J., Trotter,J.R., Peltan,A., Fleck,M. and Stuart,K. (2008) RNA editing in *Trypanosoma brucei* requires three different editosomes. *Mol. Cell Biol.*, **28**, 122–130.
- Carnes,J., Soares,C.Z., Wickham,C. and Stuart,K. (2011) Endonuclease associations with three distinct editosomes in *Trypanosoma brucei*. *J. Biol. Chem.*, **286**, 19320–19330.
- Carnes,J., McDermott,S., Anupama,A., Oliver,B.G., Sather,D.N. and Stuart,K. (2017) *In vivo* cleavage specificity of *Trypanosoma brucei* editosome endonucleases. *Nucleic Acids Res.*, **45**, 4667–4686.
- McAdams,N.M., Simpson,R.M., Chen,R., Sun,Y. and Read,L.K. (2018) MRB7260 is essential for productive protein-RNA interactions within the RNA editing substrate binding complex during trypanosome RNA editing. *RNA*, **24**, 540–556.
- McAdams,N.M., Harrison,G.L., Tylec,B.L., Ammerman,M.L., Chen,R., Sun,Y. and Read,L.K. (2019) MRB10130 is a RESC assembly factor that promotes kinetoplastid RNA editing initiation and progression. *RNA*, **25**, 1177–1191.
- Hashimi,H., Čičová,Z., Novotná,L., Wen,Y.-Z. and Lukeš,J. (2009) Kinetoplastid guide RNA biogenesis is dependent on subunits of the

- mitochondrial RNA binding complex 1 and mitochondrial RNA polymerase. *RNA*, **15**, 588–599.
29. Weng, J., Aphasizheva, I., Etheridge, R.D., Huang, L., Wang, X., Falick, A.M. and Aphasizhev, R. (2008) Guide RNA-binding complex from mitochondria of trypanosomatids. *Mol. Cell*, **32**, 198–209.
 30. Kafková, L., Ammerman, M.L., Faktorová, D., Fisk, J.C., Zimmer, S.L., Sobotka, R., Lukeš, J. and Hashimi, H. (2012) Functional characterization of two paralogs that are novel RNA binding proteins influencing mitochondrial transcripts of *Trypanosoma brucei*. *RNA*, **18**, 1846–1861.
 31. Fisk, J.C., Ammerman, M.L., Presnyak, V. and Read, L.K. (2008) TbRGG2, an essential RNA editing accessory factor in two *Trypanosoma brucei* life cycle stages. *J. Biol. Chem.*, **283**, 23016–23025.
 32. Lueong, S., Merce, C., Fischer, B., Hoheisel, J.D. and Erben, E.D. (2016) Gene expression regulatory networks in *Trypanosoma brucei*: insights into the role of the mRNA-binding proteome. *Mol. Microbiol.*, **100**, 457–471.
 33. Kumar, V., Madina, B.R., Gulati, S., Vashist, A.A., Kanyumbu, C., Pieters, B., Shakir, A., Wohlschlegel, J.A., Read, L.K., Mooers, B.H. *et al.* (2016) REH2C helicase and GRBC subcomplexes may base pair through mRNA and small guide RNA in kinetoplastid editosomes. *J. Biol. Chem.*, **291**, 5753–5764.
 34. Madina, B.R., Kumar, V., Mooers, B.H. and Cruz-Reyes, J. (2015) Native variants of the MRB1 complex exhibit specialized functions in kinetoplastid RNA editing. *PLoS One*, **10**, e0123441.
 35. Aphasizheva, I., Zhang, L., Wang, X., Kaake, R.M., Huang, L., Monti, S. and Aphasizhev, R. (2014) RNA binding and core complexes constitute the U-insertion/deletion editosome. *Mol. Cell Biol.*, **34**, 4329–4342.
 36. Kumar, V., Doharey, P.K., Gulati, S., Meehan, J., Martinez, M.G., Hughes, K., Mooers, B.H.M. and Cruz-Reyes, J. (2019) Protein features for assembly of the RNA editing helicase 2 subcomplex (REH2C) in trypanosome holo-editosomes. *PLoS One*, **14**, e0211525.
 37. Vondrušková, E., van den Burg, J., Ziková, A., Ernst, N.L., Stuart, K., Benne, R. and Lukeš, J. (2005) RNA interference analyses suggest a transcript-specific regulatory role for mitochondrial RNA-binding proteins MRP1 and MRP2 in RNA editing and other RNA processing in *Trypanosoma brucei*. *J. Biol. Chem.*, **280**, 2429–2438.
 38. Pelletier, M. and Read, L.K. (2003) RBP16 is a multifunctional gene regulatory protein involved in editing and stabilization of specific mitochondrial mRNAs in *Trypanosoma brucei*. *RNA*, **9**, 457–468.
 39. Shaw, P.L., McAdams, N.M., Hast, M.A., Ammerman, M.L., Read, L.K. and Schumacher, M.A. (2015) Structures of the *T. brucei* kRNA editing factor MRB1590 reveal unique RNA-binding pore motif contained within an ABC-ATPase fold. *Nucleic Acids Res.*, **43**, 7096–7109.
 40. Mehta, V., Moshiri, H., Srikanth, A., Kala, S., Lukeš, J. and Salavati, R. (2020) Sulfonated inhibitors of the RNA editing ligases validate the essential role of the MRP1/2 proteins in kinetoplastid RNA editing. *RNA*, **26**, 827–835.
 41. Sprehe, M., Fisk, J.C., McEvoy, S.M., Read, L.K. and Schumacher, M.A. (2010) Structure of the *Trypanosoma brucei* p22 protein, a cytochrome oxidase subunit II-specific RNA-editing accessory factor. *J. Biol. Chem.*, **285**, 18899–18908.
 42. Fisk, J.C., Presnyak, V., Ammerman, M.L. and Read, L.K. (2009) Distinct and overlapping functions of MRP1/2 and RBP16 in mitochondrial RNA metabolism. *Mol. Cell Biol.*, **29**, 5214–5225.
 43. Panigrahi, A.K., Ernst, N.L., Domingo, G.J., Fleck, M., Salavati, R. and Stuart, K.D. (2006) Compositionally and functionally distinct editosomes in *Trypanosoma brucei*. *RNA*, **12**, 1038–1049.
 44. Panigrahi, A.K., Allen, T.E., Stuart, K., Haynes, P.A. and Gygi, S.P. (2003) Mass spectrometric analysis of the editosome and other multiprotein complexes in *Trypanosoma brucei*. *J. Am. Soc. Mass Spectrom.*, **14**, 728–735.
 45. Stuart, K., Panigrahi, A.K. and Schnauffer, A. (2004) In: *RNA Interference, Editing, and Modification*. Springer, pp. 273–291.
 46. Aphasizheva, I., Yu, T., Suematsu, T., Liu, Q., Mesitov, M.V., Yu, C., Huang, L., Zhang, L. and Aphasizhev, R. (2020) Poly(A) binding KPAF4/5 complex stabilizes kinetoplast mRNAs in *Trypanosoma brucei*. *Nucleic Acids Res.*, **48**, 8645–8662.
 47. Hernandez, A., Madina, B.R., Ro, K., Wohlschlegel, J.A., Willard, B., Kinter, M.T. and Cruz-Reyes, J. (2010) REH2 RNA helicase in kinetoplastid mitochondria: ribonucleoprotein complexes and essential motifs for unwinding and guide RNA (gRNA) binding. *J. Biol. Chem.*, **285**, 1220–1228.
 48. Li, F., Herrera, J., Zhou, S., Maslov, D.A. and Simpson, L. (2011) Trypanosome REH1 is an RNA helicase involved with the 3′–5′ polarity of multiple gRNA-guided uridine insertion/deletion RNA editing. *Proc. Natl. Acad. Sci. U.S.A.*, **108**, 3542–3547.
 49. Kruse, E., Voigt, C., Leeder, W.-M. and Göringer, H.U. (2013) RNA helicases involved in U-insertion/deletion-type RNA editing. *Biochim. Biophys. Acta Gene Regul. Mech.*, **1829**, 835–841.
 50. Jarmoskaite, I. and Russell, R. (2011) DEAD-box proteins as RNA helicases and chaperones. *Wiley Interdiscip. Rev. RNA*, **2**, 135–152.
 51. Linder, P. and Jankowsky, E. (2011) From unwinding to clamping—the DEAD box RNA helicase family. *Nat. Rev. Mol. Cell Biol.*, **12**, 505–516.
 52. Missel, A., Souza, A.E., Nörskau, G. and Göringer, H. (1997) Disruption of a gene encoding a novel mitochondrial DEAD-box protein in *Trypanosoma brucei* affects edited mRNAs. *Mol. Cell Biol.*, **17**, 4895–4903.
 53. Arhin, G.K., Shen, S., Ullu, E. and Tschudi, C. (2004) A PCR-based method for gene deletion and protein tagging in *Trypanosoma brucei*. *Methods Mol. Biol.*, **270**, 277–286.
 54. Kafková, L., Tu, C., Pazzo, K.L., Smith, K.P., Debler, E.W., Paul, K.S., Qu, J. and Read, L.K. (2018) *Trypanosoma brucei* PRMT1 is a nucleic acid binding protein with a role in energy metabolism and the starvation stress response. *Mbio*, **9**, e02430-18.
 55. Wirtz, E., Leal, S., Ochatt, C. and Cross, G.M. (1999) A tightly regulated inducible expression system for conditional gene knock-outs and dominant-negative genetics in *Trypanosoma brucei*. *Mol. Biochem. Parasitol.*, **99**, 89–101.
 56. Ammerman, M.L., Hashimi, H., Novotná, L., Cicová, Z., McEvoy, S.M., Lukes, J. and Read, L.K. (2011) MRB3010 is a core component of the MRB1 complex that facilitates an early step of the kinetoplastid RNA editing process. *RNA*, **17**, 865–877.
 57. Carnes, J., Trotter, J.R., Ernst, N.L., Steinberg, A. and Stuart, K. (2005) An essential RNase III insertion editing endonuclease in *Trypanosoma brucei*. *Proc. Natl. Acad. Sci. U.S.A.*, **102**, 16614–16619.
 58. Gruber, A.R., Lorenz, R., Bernhart, S.H., Neuböck, R. and Hofacker, I.L. (2008) The ViennaRNA websuite. *Nucleic Acids Res.*, **36**, W70–W74.
 59. Koslowsky, D., Sun, Y., Hindenach, J., Theisen, T. and Lucas, J. (2014) The insect-phase gRNA transcriptome in *Trypanosoma brucei*. *Nucleic Acids Res.*, **42**, 1873–1886.
 60. Panigrahi, A.K., Gygi, S.P., Ernst, N.L., Igo, R.P., Palazzo, S.S., Schnauffer, A., Weston, D.S., Carmean, N., Salavati, R., Aebersold, R. *et al.* (2001) Association of two novel proteins, TbMP52 and TbMP48, with the *Trypanosoma brucei* RNA Editing Complex. *Mol. Cell Biol.*, **21**, 380–389.
 61. Gerasimov, E.S., Gasparyan, A.A., Kaurov, I., Tichý, B., Logacheva, M.D., Kolesnikov, A.A., Lukeš, J., Yurchenko, V., Zimmer, S.L. and Flegontov, P. (2018) Trypanosomatid mitochondrial RNA editing: dramatically complex transcript repertoires revealed with a dedicated mapping tool. *Nucleic Acids Res.*, **46**, 765–781.
 62. Sortino, K., Tylec, B.L., Chen, R., Sun, Y. and Read, L.K. (2022) Conserved and transcript-specific functions of the RESC factors, RESC13 and RESC14, in kinetoplastid RNA editing. *RNA*, **28**, 1496–1508.
 63. Aphasizheva, I. and Aphasizhev, R. (2010) RET1-catalyzed uridylylation shapes the mitochondrial transcriptome in *Trypanosoma brucei*. *Mol. Cell Biol.*, **30**, 1555–1567.
 64. Suematsu, T., Zhang, L., Aphasizheva, I., Monti, S., Huang, L., Wang, Q., Costello, C.E. and Aphasizhev, R. (2016) Antisense transcripts delimit exonucleolytic activity of the mitochondrial 3′ processome to generate guide RNAs. *Mol. Cell*, **61**, 364–378.
 65. De Bortoli, F., Espinosa, S. and Zhao, R. (2021) DEAH-box RNA helicases in pre-mRNA splicing. *Trends Biochem. Sci.*, **46**, 225–238.
 66. Schmid, B., Riley, G.R., Stuart, K. and Göringer, H.U. (1995) The secondary structure of guide RNA molecules from *Trypanosoma brucei*. *Nucleic Acids Res.*, **23**, 3093–3102.
 67. Böhm, C., Katari, V.S., Brecht, M. and Göringer, H.U. (2012) *Trypanosoma brucei* 20 S editosomes have one RNA substrate-binding site and execute RNA unwinding activity. *J. Biol. Chem.*, **287**, 26268–26277.